A phylogenetic test of adaptation to deserts and aridity in skull and dental morphology across rodents

Bader H. Alhajeri[*] and Scott J. Steppan

Department of Biological Sciences, Kuwait University, Safat, 13110, Kuwait (BHA)
Department of Biological Science, Florida State University, Tallahassee, FL 32306-4295, USA (SJS)

* Correspondent: bader.alhajeri@ku.edu.kw

Understanding how organisms adapt to aridity is a central theme in traditional desert ecology research. However, many of the pioneering studies were conducted before detailed phylogenies were available to provide evolutionary context and before the accumulation of accurate bioclimatic and species distribution data to provide geographic and environmental context. We tested the desert-adaptive value of changes in skull and dental morphology in rodents after phylogenetic correction. In addition, we estimated that across the evolutionary history of more than 2,400 rodent species, transitions between mesic and desert habitats have been very frequent, with a directional bias toward the mesic-to-desert transition. This suggested that derived desert specialization is an "evolutionary dead-end" that limits further evolution. After correcting for the strong phylogenetic signal, we still find a significant and strong correlation between habitat aridity and specializations associated with auditory sensitivity (auditory bulla inflation) and respiratory water retention (nasal passage elongation) but not in characters associated with dietary specialization (lower incisor shape). No other significant associations were found between habitat or aridity and any other cranial, jaw, or dental traits. Bullar hypertrophy is among the strongest patterns of convergent cranial desert adaptation in rodents and indicates that adaptation plays a similar role in shaping the evolution of this structure in different desert rodent clades.

Key words: adaptation, auditory bulla, convergence, desert ecology, habitat transition, nasal, specialization, tooth

Understanding how organisms adapt to their environment is a central theme in traditional ecological research, where morphology is assumed to reflect both habitat-specific adaptations (Wainwright and Reilly 1994) and phylogenetic history. This is especially true for convergent desert adaptations in rodents, including those for fossoriality and bipedality, but mostly adaptations to water and energy conservation that enable rodents to survive these extreme habitats (Vial 1962; Mares 1975, 1976). Rodents are particularly amenable to studies of adaptation because they are speciose, found on all continents except Antarctica, and occupy variable habitats ranging from mesic rainforests to arid deserts (Fabre et al. 2012).

Deserts constitute the largest terrestrial biome, covering one-fifth of dry land (Hickman et al. 2004), and while varying greatly in temperature, are defined by their aridity that is caused by low and unpredictable rainfall that erodes the soil (Louw and Seely 1982). Adaptations to deserts are either directly to aridity or indirectly to the habitat manifestations of aridity such as low plant cover (where perennials cover less than 10% of total area) and low food and water resources most of the year (Sowell 2001; Ward 2009). Desert adaptations also include those in response to predation pressures, such as the reoccurring evolution of camouflage in desert rodents that allows them to evade detection (Boratyński et al. 2017).

Among the most studied convergent desert-adaptive structures in mammals, also characteristic of fossorial species, is the hypertrophied auditory bulla (especially the tympanic and mastoid cavities), which is a bony cranial chamber that houses the middle ear bones and amplifies low-frequency sounds (e.g., kangaroo rats, *Dipodomys* spp.—Webster and Webster 1975; gerbils, Gerbillinae—Lay 1972; Alhajeri et al. 2015; Mason 2015; Neotropical spiny rats, Echimyidae—Gardner and Emmons 1984; mole-rats, Bathyergidae—Burda et al. 1989; marsupial moles, *Notoryctes* spp.—Mason 2001; sand cats, *Felis margarita*—Huang et al. 2002; tuco-tucos, *Ctenomys* spp.—Francescoli 1999; Schleich and Vasallo 2003; Francescoli et al. 2012; golden moles, Chrysochloridae—Mason 2003; armadillos, Dasypodidae—Squarcia et al. 2007; jerboas,

Dipodidae—Mason 2015; and sengis, Macroscelididae—Mason 2015). In a comparison of 13 gerbil species, Lay (1972) found that more arid environments are correlated with increased anatomical specialization of middle and inner ear anatomy and as a consequence, increased auditory sensitivity. The increased auditory sensitivity that accompanies auditory bulla enlargement is described as an adaptation for both prey capture and predator avoidance in open habitats where sound dissipates quickly and early detection is key to escape more effective predators (Lay 1972; Webster and Webster 1975). Many desert rodents are fossorial, because open habitats have few natural shelters and increased sound sensitivity is important for subterranean vocalizations that use low-frequency sounds (Lay 1972; Webster and Webster 1975).

Internal nasal passage (turbinate) morphology has been proposed to be an adaption to aridity (Feldhamer et al. 2007). Longer, narrower, and more convoluted turbinates are more efficient at cooling exhaled air and therefore better in water conservation through condensation and reabsorption of exhaled air (e.g., kangaroo rats—Schmidt-Nielsen and Schmidt-Nielsen 1950; degus, *Octodon degus*—Cortes et al. 1988, 1990). Agrawal (1967) showed that there is a tendency of decreased nasal length as a digging adaptation in fossorial rodents because projecting nasals hinder burrowing and have a greater chance of injury, which could confound the potential relationship in rodents, because most desert species are fossorial.

Finally, broad and short lower incisors have been proposed to be an adaption to remove salt from desert saltbush epidermis in various rodent groups (Ojeda et al. 1999). However, subsequent studies have not tested the association between incisor shape and aridity in a large sample of rodent species.

Here, we test the adaptive value of the auditory bulla, nasal morphology, and lower incisor shape on a broad taxonomic scale that includes desert and mesic representatives from most rodent families. Most comparative morphological studies of desert adaptation are based on very limited taxonomic sampling and small sample sizes, and most of the documented associations with deserts have been anecdotal and not rigorously tested. We use an order-level molecular phylogeny of rodents to correct correlation tests for evolutionary relationships. We test the association between 5 putatively adaptive morphological traits (bullar index [BI], bullar volume [BV], lower incisor index [LII], nasal index [NI], and nasal volume [NV]) with 4 measures of aridity.

Questions and Hypotheses

Our principal question is: 1) are the auditory bulla, lower incisor, and nasal morphologies in rodents desert-adaptive? We predict that increased aridity (decrease in aridity index, decrease in mean annual precipitation, and increase in mean annual temperature) will be directly correlated with an: a) increase in both BI and BV, reflecting an increase in absolute and relative size; b) increase in LII, indicating a "squarer" shape; and c) decrease in both NI and NV, reflecting longer and narrower nasal passages that are more efficient at water conservation of exhaled air. We also ask: 2) is some variation in other aspects of skull morphology, not previously hypothesized to be desert-adaptive (henceforth "desert-neutral" traits; based on standard skull measurements), also correlated with aridity? Finally, we quantify: 3) the pattern of transition between mesic and desert habitats, using all extant rodent species and ancestral state reconstruction.

Materials and Methods

Composite rodent chronogram.—We used a chronogram adapted from Fabre et al. (2012) that includes all extant rodent species. Fabre et al.'s (2012) tree was estimated using maximum likelihood (ML) from a supermatrix of 11 mitochondrial and nuclear genes of 1,265 rodent species and multiple fossil calibrations. The superfamily Muroidea was pruned from Fabre et al.'s (2012) tree and replaced with Steppan and Schenk's (2017) muroid chronogram that included more species, was based primarily on nuclear sequences, and excluded misidentified sequences found in Fabre et al. (2012). We maintained the crown age for muroids from Steppan and Schenk's (2017) tree at 32.6 million years ago (Ma) and the stem age from Fabre et al.'s (2012) tree at 48.77 Ma, retaining the ultrametricity of the chronogram.

Species lacking molecular data were grafted onto the tree closest to the species that shares the most recent common ancestor (e.g., same genus, same subfamily) based on the taxonomy of Carleton and Musser (2005), resulting in a tree with 2,357 species. If morphological and habitat data were obtained from more than 1 subspecies, then the species tip was split midbranch, creating polytomies, and data were applied separately to each tip in subsequent analyses, conducted using a final tree that includes 2,414 operational taxonomic units (OTUs). Tree pruning, grafting, and ultrametricity checks were conducted in the Ape library (Paradis et al. 2004) in R (R Development Core Team 2013).

Binary habitat categories and quantification of habitat transition.—All 2,414 OTUs were classified as desert or mesic based on the information from the literature (Supplementary Data SD1), primarily using information from the International Union for Conservation of Nature Red List (IUCN 2013) following Alhajeri et al. (2015) and Alhajeri and Steppan (2016). In addition to this classification scheme, analyses were also conducted on a classification based on Shenbrot et al. (1999) and results of the 2 schemes were compared (see Alhajeri et al. 2015).

The frequency and pattern of transition between desert and mesic environments were estimated using ancestral character reconstruction using both ML, as implemented in the Ape library, and Bayesian stochastic character mapping (BS—Huelsenbeck et al. 2003) as implemented in the Phytools library (Revell 2012) in R using binary habitat categories ("desert" versus "mesic") derived from IUCN (2013). Stochastic character mapping in Phytools is based on the method described in SIMMAP (Bollback 2006). Both ML and BS approaches used the all rates different matrix (ARD) 2-parameter model (with different rates

estimated for forward and reverse transitions). ARD fits the data significantly better than both the equal rates (ER) 1-parameter model and the symmetric (SYM) 1-parameter model (same rate estimated for forward and reverse transitions; ER and SYM are identical for binary traits), as determined by the likelihood ratio test (ΔlnL = 36.98, P < 0.0001).

Habitat transitions in ML were inferred as occurring along the branch where the ancestral node is more likely (> 50%) to be 1 habitat type (e.g., mesic) and the descendant node is most likely (> 50%) to be another habitat type (e.g., desert). The BS analysis used the best-fit evolutionary model (ARD) and tip states (desert versus mesic) to simulate stochastic character histories of the habitat using the fitted continuous time-reversible Markov model of evolution (Huelsenbeck et al. 2003; Revell 2012). Habitat transition rates were based on the average of 1,000 history maps.

Extraction of continuous environmental data.—The typical climatic conditions encountered by each species were based on the mean of the of bioclimatic variables across each species' geographical range, which were extracted from the WORLDCLIM database (www.worldclim.org—Hijmans et al. 2005) at a spatial resolution of 2.5 min, using DIVA-GIS 7.5 (Hijmans et al. 2012) following Alhajeri et al. (2015) and Alhajeri and Steppan (2016).

The average of each bioclimatic variable was calculated across the range of each species by averaging each grid cell observation that falls within each species' polygon shape file, which were downloaded from IUCN (2013). Mean annual temperature and mean annual precipitation were extracted for comparative analyses in addition to average temperature and precipitation of the driest quarters, which were used to calculate the aridity index (Supplementary Data SD2 and SD3) following the method of De Martonne (1927, 1942), using the modifications described previously in Alhajeri et al. (2015). The aridity index is unitless, ranging from 0 to 60 for most habitat types, with lower values indicating increased aridity (Lungu et al. 2011). By incorporating both precipitation and temperature variables (Supplementary Data SD3), this index can be used as a proxy for potential evapotranspiration, with temperature used as a measure of evaporation capacity (Maliva and Missimer 2012), and thus captures water availability as a function of temperature and precipitation (Baltas 2007).

To meet the assumptions of normality of subsequent analyses, both mean annual precipitation and the aridity index scores were log transformed. Fifteen species with negative (raw) aridity index scores were dropped (see Alhajeri et al. 2015 for details) because De Martonne's (1927, 1942) aridity index does not vary monotonically when mean annual temperature or the mean temperature of the driest quarter (Supplementary Data SD3) is lower than −10°C, resulting in artifactually inflated negative scores (Supplementary Data SD2), regardless of the precipitation values. Negative values do not accurately reflect aridity in such situations; in fact, the constant (10°C) is added to the denominators to avoid negative values in very cold regions (Lungu et al. 2011). We also dropped 5 outlier species with extremely high aridity index scores (> 200) because these

scores were several orders of magnitude greater than most of the species in the sample (Supplementary Data SD2), as a consequence of occurring in extremely mesic regions with very high precipitation values. The exclusion of these species did not qualitatively change the results of the analysis. However, their inclusion in the dataset would violate the normality of residuals assumption of the phylogenetic generalized least squares (PGLS) analysis, which is especially affected by residual distributions consisting of a few large outliers (Mundry 2014).

Morphological data collection.—We examined 1–9 specimens from 591 rodent OTUs (species or subspecies), for a total of 2,075 specimens (Appendix I). Where possible, equal numbers of males and females were measured, although sexual dimorphism is uncommon in rodents. We sampled most of the available desert rodent species present in the museums listed below, in addition to a selection of close mesic relatives, to maximize our power to detect desert adaptation. All 5 rodent suborders and 79% of the families were sampled, including all families with any desert species.

Morphological measurements were obtained from the skulls of voucher specimens from the collections of the American Museum of Natural History (AMNH) in New York, the Field Museum of Natural History (FMNH) in Chicago, the Museum of Vertebrate Zoology (MVZ) in Berkeley, California, the United States National Museum of Natural History in Washington, D.C. (USNM), the University of Florida Museum of Natural History (FLMNH) in Gainesville, Laboratorio de Citogenética de Mamíferos, Universidad de Chile (LCM) in Chile, and the Sam Noble Oklahoma Museum of Natural History (SNOMNH). Only wild-caught adult individuals were chosen. Adult status was assessed by the basioccipital–basisphenoid epiphyseal fusion as in Robertson and Shadle (1954) and Samuels (2009) as well as the complete eruption of 3rd molars, reaching the occlusal surface (Steppan 1997).

Skull measurements were extracted from photographs captured with a Nikon D3200 digital SLR camera using a Nikon 40 mm f/2.8G AF-S DX Micro-Nikkor Lens (Nikon, Tokyo, Japan) at 6,016 × 4,000 resolution in a standardized manner. Up to 10 photographs were taken per individual and included multiple magnifications of the dorsal, ventral, and lateral orientations of the skull, with a scale bar included in each photograph. All measurements were taken from images of the left side of the skull using TpsDig v2.16 (Rohlf 2010). If the left side of the skull was damaged, the right side was measured instead.

Species averages were calculated for all morphological characters from distances extracted from the ventral (Supplementary Data SD4 and SD5), lateral (Supplementary Data SD6 and SD7), and dorsal (Supplementary Data SD6 and SD8) views of crania as well as the occlusal (Supplementary Data SD9 and SD10) and lateral (Supplementary Data SD9 and SD11) views of the mandibles. Distances observable from multiple views of the crania or mandibles were measured in all views, and averaged, before calculating subsequent derivative characters, such as bulla volume and NI (Supplementary Data SD12) to reduce the effects of flattening a 3D structure to 2D images. The 47 measurements obtained from each skull are

described in Appendix II. All morphological variables were log transformed prior to subsequent phylogenetic or size correction (see below). Five shape indices, assumed to represent morphological adaptations to aridity, were calculated as: BI = bulla length divided by skull length; BV = product of length, width, and depth; NI = breadth divided by length; NV = product of breadth, length, and rostral depth; LII = width divided by length (see Appendix II for more detailed descriptions).

Phylogenetic and size correction.—Phylogenetic signal was computed by calculating the *K*-statistic under a Brownian motion (BM) model of evolution with statistical significance calculated via 1,000 randomizations (Blomberg et al. 2003); values close to zero indicate no phylogenetic signal (close relatives do not look more similar than distant relatives), $K = 1$ indicates resemblance of relatives predicted by BM, and $K > 1$ indicates more resemblance than expected by BM (Blomberg et al. 2003).

Distances were scaled by size using shearing, calculated as the residuals from a least squares regression analyses of each trait against the 1st principal component of the pooled data, the latter used as a size measure (McCoy et al. 2006).

We tested the correlation between environmental and morphological variables, both with and without correcting for phylogeny. The tree used in phylogenetic correction contained 591 OTUs (Fig. 1; Supplementary Data SD13 and SD14) extracted from the 2,414 OTU rodent phylogeny described above. Shearing and principal component analysis (PCA) were conducted *after* correcting for phylogenetic non-independence among species. This is important because not accounting for phylogeny at the preliminary transformations can increase variance and type I error, even if phylogeny was accounted for in subsequent analyses, leading to spurious results in phylogenetic comparative methods (Revell 2009). Phylogenetic signal calculation, phylogenetic size correction, and phylogenetic PCA were conducted following Revell (2009) using the Phytools library in R.

Univariate analyses of putative desert-adaptive characters.—The association between the 5 morphological indices with climate and habitat data was tested in a univariate framework as follows. Data where only size correction was performed were tested for desert adaptation by conducting generalized least squares analyses of each character onto the aridity index, mean annual temperature (BIO1), and mean annual rainfall (BIO12). These regressions were conducted on each climatic variable separately. In addition, an analysis of variance
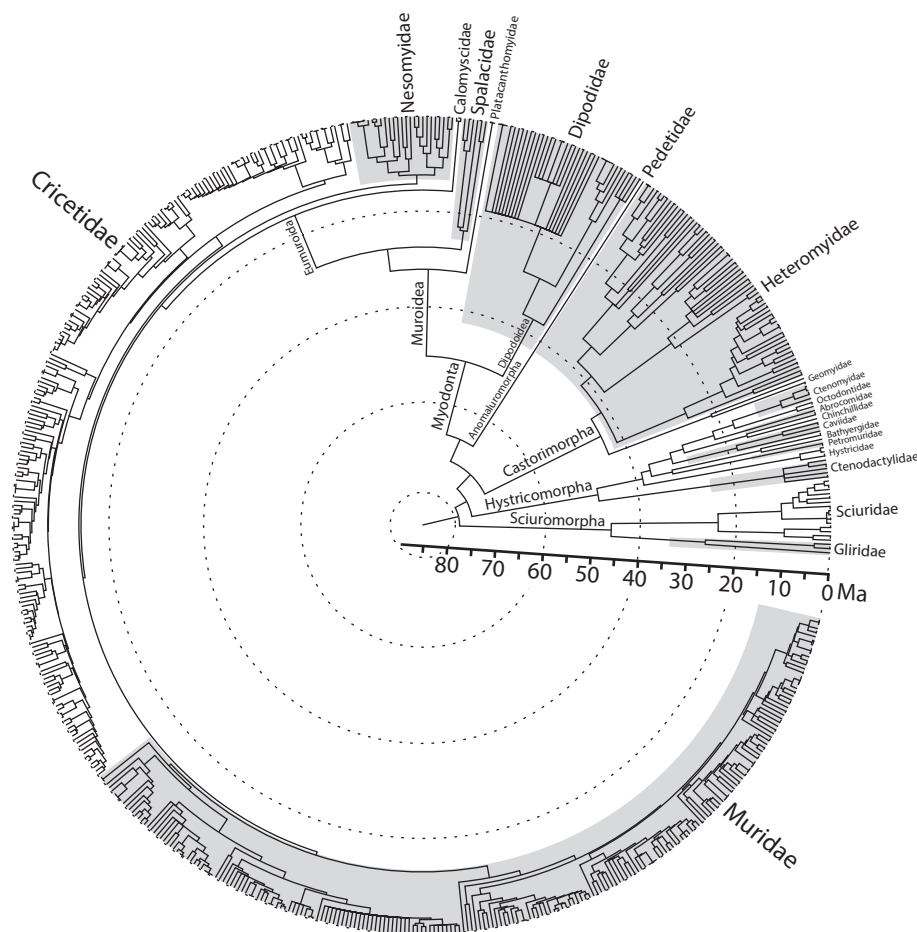
Fig. 1.—Summarized composite chronogram of 591 rodent operational taxonomic units (OTUs) with collected morphological data. Molecular phylogeny modified from Fabre et al. (2012) and Steppan and Schenk (2017). Major taxonomic groups are indicated. Desert and mesic species are indicated in Supplementary Data SD13 and species labels are in Supplementary Data SD14. Trees summarizing results of ancestral state reconstruction are in Supplementary Data SD15 and SD16.

(ANOVA) was conducted while classifying species as desert or mesic using IUCN data (Supplementary Data SD1). Both these analyses were conducted in the R base package.

Data where both size and phylogenetic correction was performed were tested for desert adaptation by conducting PGLS analyses of each character onto the 3 bioclimatic variables following the method of Freckleton et al. (2002). PGLS was used instead of independent contrasts because it can tolerate polytomies better. Analyses on discrete data (desert versus mesic) were conducted using phylogenetic ANOVA (PhyANOVA) with 1,000 phylogenetic simulations following the method of Garland et al. (1993). PhyANOVA was conducted in the Phytools library and PGLS was conducted using the Caper library (Orme et al. 2013) in R.

Multivariate analyses of overall skull morphology.—To test the generality of skull adaptation to deserts in rodents, the association between a suite of 29 standard linear measurements intended to capture overall skull morphology (not including the putative desert-adaptive characters tested above) with climate and habitat data was tested in a multivariate framework as follows: 1) Morphological data were subjected to PCA and the first 6 principal components were inspected for separation of desert versus mesic rodents in all 3 datasets (raw, size corrected, and phylogenetic size corrected). 2) A discriminant function analysis (DFA) was performed to provide information as to the relative contribution of each morphological variable in the discrimination between these 2 groups. 3) A multivariate analysis of variance (MANOVA) was performed to see if these 2 groups have significantly different overall morphologies. Non-phylogenetic PCA was conducted using singular value decomposition in the PcaMethods library (Stacklies et al. 2007), phylogenetic PCA was conducted in the Phytools library, linear DFA was conducted in the Mass library (Venables and Ripley 2002), and phylogenetic MANOVA (PhyMANOVA) was conducted in the Geiger library (Harmon et al. 2008) in R. 4) The correlation between continuous climatic variables and morphological variables was also tested using canonical correlations analyses (CCAs). CCA calculates a set of canonical variates that are orthogonal linear combinations of the variables within each set that have the maximum correlation with each other (Härdle and Simar 2012). CCA was conducted in both the Cca library (González et al. 2008) and the Yacca library (Butts 2012) in R. CCA also used code from the UCLA: Statistical Consulting Group (2013).

Results

Habitat transition in rodents.—Results from analyses using Shenbrot et al.'s (1999) habitat classification were largely concordant with those from the IUCN habitat scheme (data not shown); therefore, only analyses using the latter are presented here.

Both the ML and the BS ancestral state reconstructions on the entire rodent tree showed marginal support for the ancestral habitat of rodents being desert (SL = 52.8%, PP = 0.51). SL refers to the scaled (or proportional) likelihood of an ancestral

state (Supplementary Data SD15) and PP is the posterior probability for a given state (Supplementary Data SD16). The BS analysis estimated an average of 276.6 transitions between habitats (mesic to desert = 141.7, desert to mesic = 134.9) with 85% more time spent in the mesic habitat. Similarly, the ML analysis detected a faster forward transition rate from mesic to desert (0.073 ± 0.0074) than the reverse desert to mesic transition rate (0.013 ± 0.0011).

Difference in climate between desert and mesic environments.—Desert species faced significantly more aridity than mesic species (0.97 ± 0.41 versus 1.54 ± 0.42; $t_{1,589} = 13.82$, $P < 0.0001$; Fig. 2a), lower mean annual precipitation (2.43 ± 0.28 ln mm versus 2.97 ± 0.33 ln mm; $t_{1,589} = 17.98$, $P < 0.0001$; Fig. 2b), and lower average mean annual temperatures (16.9 ± 5.62°C versus 18.2 ± 6.64°C; $t_{1,589} = 2.18$, $P = 0.03$; Fig. 2c). This 1.3°C difference illustrates that many deserts are cold with aridity being the main criterion for classifying a region as desert.

Dataset comparison and phylogenetic signal.—The results of the 1) non-size, non-phylogenetically corrected data; the 2) size-corrected, non-phylogenetically corrected data; and the 3) size-corrected, phylogenetically corrected data are consistent in both the univariate analyses of the 5 putative desert-adaptive traits, and the multivariate analyses of the 29 desert-neutral characters.

The addition of size correction tends to reduce the significance of the correlations, and the addition of phylogenetic correction tends to reduce it even more. All non-size and size-corrected morphological data and environmental variables showed statistically significant phylogenetic signal at $P < 0.001$ and K values ranging from 0.015 to 0.66. The only exceptions were LIW (width across both lower incisors) and LII for the size-corrected dataset ($P = 0.3$, $K = 0.01$ and $P = 0.15$, $K = 0.23$, respectively); however, results in subsequent analyses were consistent with phylogenetically corrected data. In accordance with these results, only size- and phylogenetically corrected data are presented below.

Contrasts of putative desert-adaptive traits with habitat and environmental data.—PhyANOVA indicated that desert rodents have significantly greater BI scores than mesic rodents ($F = 141.39$, $P = 0.001$; Fig. 3a) indicating greater relative bulla size. PGLS indicated that BI scores were weakly but significantly negatively correlated with both aridity index (coefficient = −0.012, $R^2 = 0.008$, $P = 0.028$; Fig. 3b) and mean annual precipitation (coefficient = −0.034, $R^2 = 0.034$, $P < 0.0001$; Fig. 3c) indicating relative bulla size increased with more arid and lower rainfall environments. PGLS indicated that BI scores were not significantly correlated with mean annual temperature (coefficient = −0.0003, $R^2 = 0.001$, $P = 0.509$; Fig. 3d). The same patterns were observed in BV: PhyANOVA ($F = 162.28$, $P = 0.001$; Supplementary Data SD17a), PGLS aridity index (coefficient = −0.038, $R^2 = 0.019$, $P = 0.001$; Supplementary Data SD17b), PGLS mean annual precipitation (coefficient = −0.069, $R^2 = 0.027$, $P = 0.0001$), and PGLS mean annual temperature (coefficient = −0.00005, $R^2 = 0.002$, $P = 0.963$; Supplementary Data SD17d).

Nasal size and shape showed a more complex pattern. PhyANOVA indicated NI scores were not significantly different between desert and mesic rodents ($F = 4.29$, $P = 0.669$; Fig. 4a). However, PGLS indicated that NI scores were significantly positively correlated with aridity index (coefficient = 0.016, $R^2 = 0.008$, $P = 0.024$; Fig. 4b) and trended negatively with mean annual temperature (coefficient = −0.001, $R^2 = 0.005$, $P = 0.057$; Fig. 4d), indicating that nasals were proportionately longer and narrower in more arid and warmer environments, but not with mean annual precipitation (coefficient = 0.019, $R^2 = 0.004$, $P = 0.084$; Fig. 4c). PhyANOVA indicated that desert rodents had significantly lower NVs than mesic rodents ($F = 84.11$, $P = 0.002$; Fig. 5a). PGLS indicated that NV scores are significantly positively correlated with aridity index (coefficient = 0.026, $R^2 = 0.019$, $P = 0.001$; Fig. 5b) and mean annual precipitation (coefficient = 0.044, $R^2 = 0.023$, $P = 0.0003$; Fig. 5c), but not mean annual temperature (coefficient = −0.0005, $R^2 = 0.001$, $P = 0.544$; Fig. 5d), indicating rostra were smaller in drier environments, irrespective of temperature.

Lower incisor indices were not significantly associated with any of these habitat variables: PhyANOVA ($F = 2.34$, $P = 0.778$; Supplementary Data SD18a), PGLS aridity index (coefficient = −0.026, $R^2 = 0.002$, $P = 0.139$; Supplementary Data SD18b), mean annual precipitation (coefficient = −0.016,
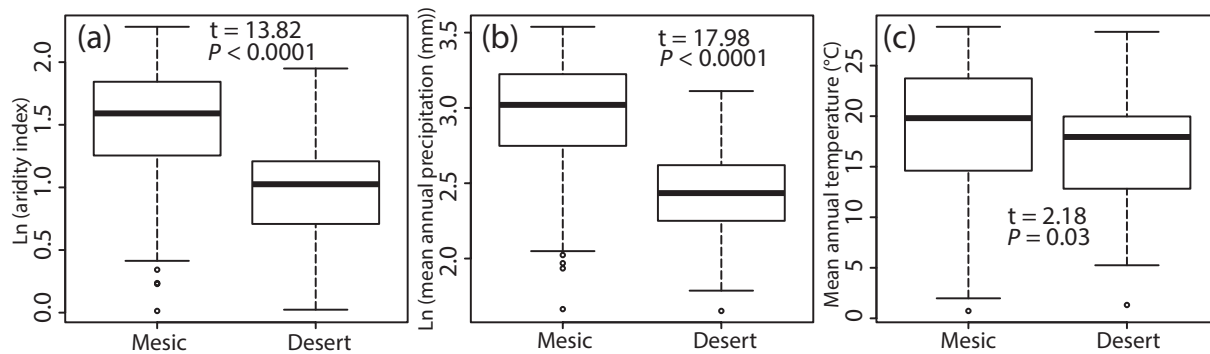
Fig. 2.—Association between binary habitat data with (a) aridity index (unitless), (b) mean annual precipitation in millimeters, and (c) mean annual temperature in °C. Indicated statistics are based on a t-test. Inner boxplot lines are median values, box margins are 25th and the 75th percentiles, whiskers are 5th and 95th percentiles, and points beyond the whiskers are outliers.
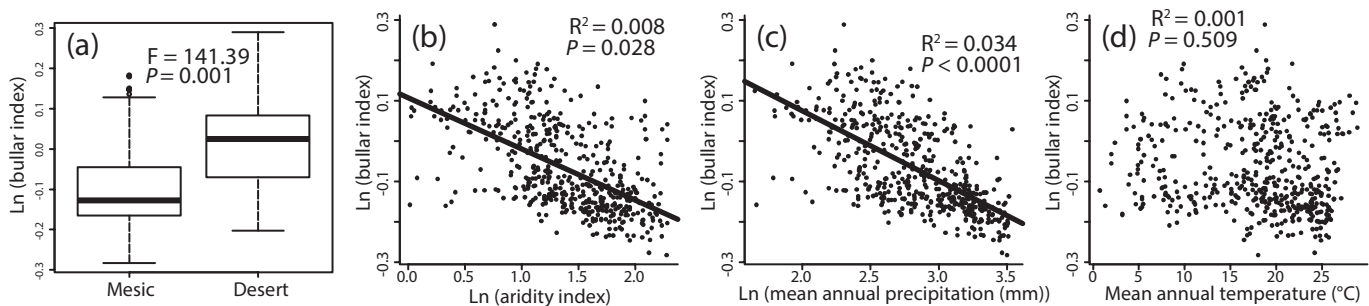
Fig. 3.—Association between bulla index scores with (a) habitat, (b) aridity index, (c) mean annual precipitation, and (d) mean annual temperature. The association between morphological variables with the binary habitat data was tested using phylogenetic analyses of variance (PhyANOVA), whereas the association with continuous environmental variables were tested using phylogenetic generalized least squares (PGLS). Boxplots and scatterplots indicate phylogenetic and size-corrected residuals of morphological variables. Indicated R^2 values, as in the text, are adjusted for the number of explanatory terms in the model relative to the number of data points (more conservative than unadjusted R^2). A best-fit line is only included in significant and marginally significant regressions.
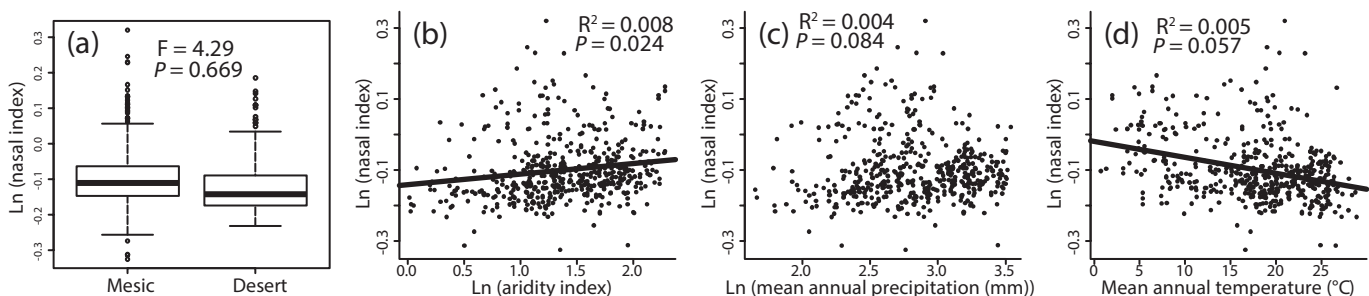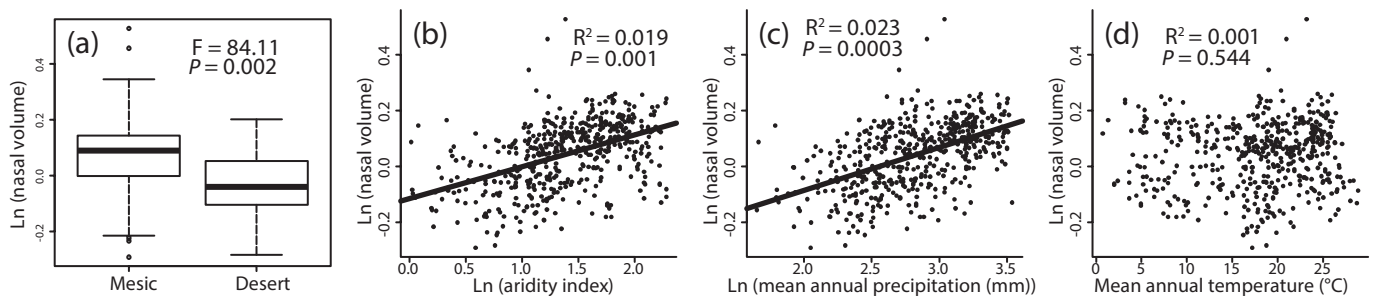

Fig. 4.—Association between nasal index scores with (a) habitat, (b) aridity index, (c) mean annual precipitation, and (d) mean annual temperature. See Fig. 3 legend for additional information.

$R^2 = 0.001$, $P < 0.563$; Supplementary Data SD18c), or mean annual temperature (coefficient = −0.002, $R^2 < 0.001$, $P = 0.311$; Supplementary Data SD18d).

Multivariate association of overall skull morphology with habitat and environment.—The morphospace represented by the first 6 size-corrected, phylogenetic principal components (extracted from 29 characters) did not clearly separate species based on binary habitat classification (Supplementary Data SD19 and SD20). Similarly, based on a visual inspection of the sole linear discriminate function, there does not seem to be clear separation between desert and mesic groups (Supplementary Data SD21 and SD22). Despite this result, the reclassification of species based on the discriminant function was highly successful with 82% of all species being correctly classified into their original habitat categories in the original dataset and 79% of correct reclassification based on the cross-validated dataset using jackknife resampling (Supplementary Data SD23). In contrast, PhyMANOVA, indicated the 2 groups were not significantly different (Wilks' $\lambda_{1,589} = 0.65$, $P = 0.96$), unlike the non-phyMANOVA, which did find a significant difference ($F_{1,589} = 8.65$, $P < 0.0001$). These results suggest that the DFA recovered clades rather than habitat groups. Taken together, the phylogenetic results indicate that desert and mesic species did not differ significantly in the 29 desert-neutral characters.

CCA indicated strong associations between the multivariate morphological and the climatic variables in all 3 dimensions

(Cor1 = 0.598, $R^2 = 0.079$, $P < 0.0001$, Fig. 6a; Cor2 = 0.500, $R^2 = 0.378$, $P < 0.0001$, Fig. 6b; Cor3 = 0.430, $R^2 = 0.187$, $P < 0.0001$, Fig. 6c). The canonical coefficients of the 1st dimension indicated that it was most strongly associated with the climate variables aridity index (0.97) and mean annual precipitation (0.89), and morphological variables bulla length (−0.78), height (−0.78), and width (−0.71) in the negative direction, and basicranial width (0.77) and incisor width (0.72) in the positive direction (Fig. 7a; Table 1). Therefore, the strongest association between these 2 datasets was a negative correlation between increased aridity index and mean annual precipitation (more mesic environments) with decreased bulla dimensions and increased basicranial width and incisor breadth. However, all other morphological variables, except for bulla length, width, and height as well as interorbital breadth and 1st molar width, were also positively associated with aridity and precipitation. The 2nd canonical dimension, which explained residual variation, was most strongly associated with the climate variables temperature (0.98) and weakly with mean annual precipitation (0.45) and the morphological variables skull length (0.51), pterygoid length (0.47), incisor depth (0.46), and nasal length (0.40) (Fig. 7b; Table 1). The residual variation explained by the 3rd canonical dimension, while significant, was weak and indicated mostly correlations among the morphological variables and not environmental variables (Fig. 7c; Table 1).

Fig. 5.—Association between nasal volume scores with (a) habitat, (b) aridity index, (c) mean annual precipitation, and (d) mean annual temperature. See Fig. 3 legend for additional information.
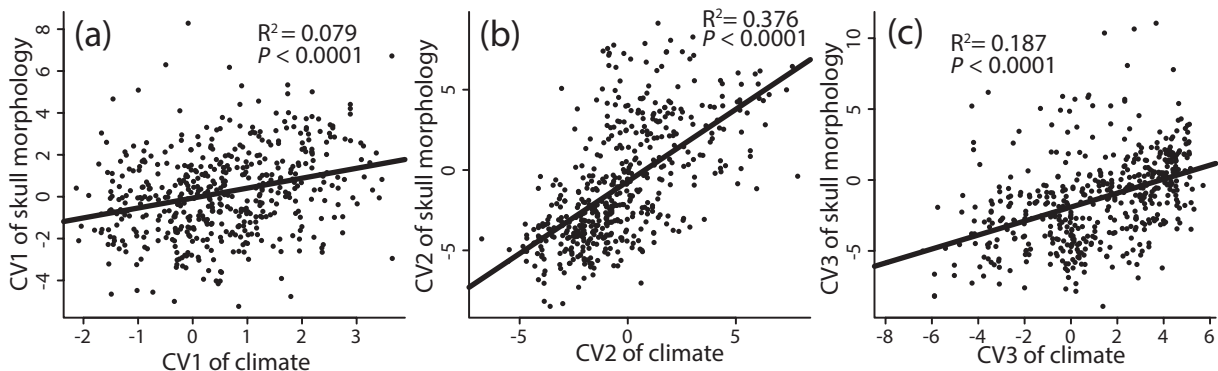
Fig. 6.—Canonical correlations of climate (mean annual precipitation, mean annual temperature, and the aridity index) versus skull morphology (29 desert-neutral characters) in 3 dimensions (a, b, and c). R^2 values and best-fit line are results of regressions of the canonical scores in the indicated dimensions (not canonical correlations, which are based on multiple dimensions, see text). CV = canonical variate.
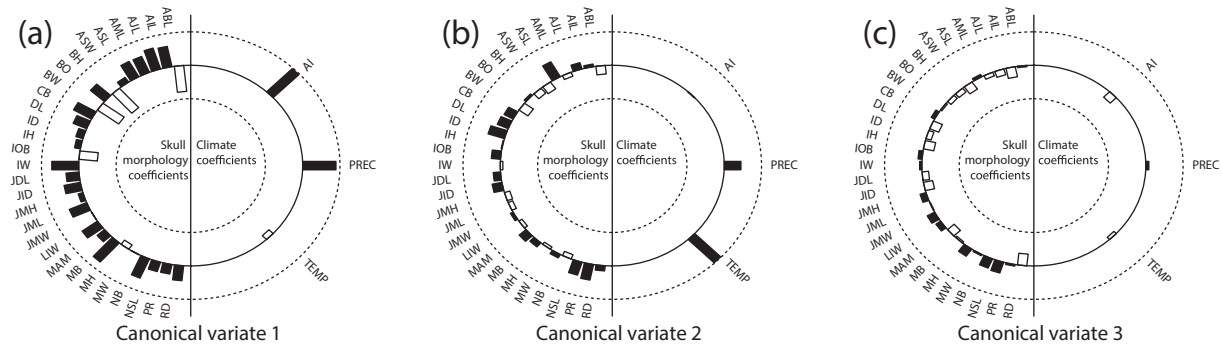
Fig. 7.—Canonical coefficients of correlations between climate (log mean annual precipitation [PREC], mean annual temperature [TEMP], and the log aridity index [AI]) and skull morphology (29 desert-neutral characters) in all 3 dimensions displayed in a circular fashion (a, b, and c). Larger (positive) values are indicated by the radial bars that are pointing outward from the base of the inner circle and the smaller (negative) values are pointing inward. ABL = average bulla length; AIL = average incisor length; AJL = average jaw length; AML = average molar length; ASL = average skull length; ASW = average skull width; BH = bulla height; BO = basioccipital length; BW = bulla width; CB = condyle breadth; DL = diastema length; ID = incisor depth; IH = incisor height; IOB = interorbital breadth; IW = incisor width; JDL = jaw diastema length; JID = jaw incisor depth; JMH = jaw 1st molar height; JML = jaw molar tooth row length; JMW = jaw 1st molar width; LIW = width across both lower incisors; MAM = moment arm masseter; MB = basicranial width; MH = 1st molar height (hypsodonty measurement); MW = 1st molar width; NB = nasal breadth; NSL = nasal length; PR = pterygoid region length; RD = rostral depth.

DISCUSSION

Habitat transition and desert specialization in rodents.—Rodents have a broad niche, a distinctive skull morphology, and specialized masticatory apparatus (i.e., incisors—Nowak 1999). Deserts are commonly described as extreme habitats, and desert rodents, with their common suite of convergent adaptations, including those for fossoriality, bipedality, water conservation, and energy conservation, are considered extremely specialized (Vial 1962; Lay 1972; Mares 1975, 1976). The BS analysis indicates that rodents spent 85% more evolutionary time in the mesic habitat state and that the desert lineages are concentrated near the tips of the tree, indicating frequent, recent desert transitions. The strong bias favoring transition from mesic to desert ecosystems in the ML analysis (5.6-fold difference) and the weak bias in the BS analysis (1.1-fold difference) indicate that it is easier for rodent lineages to transition from mesic to desert ecosystems than the reverse. This bias may also be influenced by the expansion of deserts during the Cenozoic.

Desert adaption in the auditory bulla, lower incisors, and nasals.—The association between desert habitats and enlarged bullae, squarer-shaped lower incisors, and longer and more complex nasal passages in rodents has been argued in multiple studies (e.g., Schmidt-Nielsen and Schmidt-Nielsen 1950; Lay 1972; Webster and Webster 1975; Cortes et al. 1988, 1990; Ojeda et al. 1999). However, most of these studies were descriptive, based on limited taxonomic sampling, had small sample sizes, and do not correct for phylogenetic relationships. Here, we present a quantitative, phylogenetically correct, order-level investigation of desert adaptation in skull morphology in rodents. The results show that while morphological variations of the bullae, lower incisors, and nasals have significant phylogenetic signal, phylogeny alone does not completely explain interspecific variation.

Auditory bullae are relatively larger in desert than in mesic rodents, and its size increases with increasing aridity, confirming the hypotheses from earlier, non-phylogenetic, studies (e.g., gerbils—Lay 1972; Pavlinov and Rogovin 2000; Momtazi et al. 2008; heteromyids—Webster and Webster 1975; Randall 1993; sand cats—Huang et al. 2002; Xenarthra—Squarcia et al. 2007). Enlarged auditory bullae are correlated with improved hearing of low-frequency sounds in desert and subterranean rodents (e.g., gerbils—Lay 1972; kangaroo rats—Webster and Webster 1975; Neotropical spiny rats—Gardner and Emmons 1984; tuco-tucos—Francescoli 2000; caviomorphs—Schleich and Vasallo 2003). Improved hearing at low-frequency bands is especially useful for desert rodents because deserts are open habitats where sound dissipates quickly, and increased auditory sensitivity improves both prey capture and predator avoidance rates (Lay 1972; Webster and Webster 1975) as well as conspecific communication in burrows (Francescoli et al. 2012).

Bullar hypertrophy has been described as both a desert and a fossorial adaptation, sometimes in the same species. This is unsurprising because many desert rodents are fossorial (e.g., gerbils—Lay 1972; tuco-tucos—Francescoli et al. 2012) because deserts are open habitats with relatively few natural shelters (Lay 1972) and burrows provide refuge from fatally high daytime temperatures in some regions; burrows are also moister, which facilitates water conservation (Ward 2009). We found bullar hypertrophy in desert rodents despite the inclusion of fossorial species that achieve enhanced low-frequency hearing through adaptations of the inner ear, without the inflation of the auditory bulla (e.g., naked mole-rats, *Heterocephalus glaber*—Heffner and Heffner 1992). Naked mole-rats appear to be the exception to the trend of bullar hypertrophy in fossorial desert rodents—a constraint on the size of the auditory bulla resulting from the mandible functioning in tooth-digging has been described for another fossorial group, the tuco-tucos (Verzi and Olivares 2006).

Lower incisor shape does not appear to be associated with habitat or any other climatic variables, either with or without phylogenetic or size correction. The association between this

Table 1.—Canonical coefficient values of correlations between climate (mean annual precipitation, mean annual temperature, and the aridity index) and skull morphology (29 desert-neutral characters) in all 3 dimensions. See Fig. 7 for more information. PREC = log mean annual precipitation; TEMP = mean annual temperature. ABL = average bulla length; AIL = average incisor length; AJL = average jaw length; AML = average molar length; ASL = average skull length; ASW = average skull width; BH = bulla height; BO = basioccipital length; BW = bulla width; CB = condyle breadth; DL = diastema length; ID = incisor depth; IH = incisor height; IOB = interorbital breadth; IW = incisor width; JDL = jaw diastema length; JID = jaw incisor depth; JMH = jaw 1st molar height; JML = jaw molar tooth row length; JMW = jaw 1st molar width; LIW = width across both lower incisors; MAM = moment arm masseter; MB = basicranial width; MH = 1st molar height (hypsodonty measurement); MW = 1st molar width; NB = nasal breadth; NSL = nasal length; PR = pterygoid region length; RD = rostral depth.

	Canonical variate 1	Canonical variate 2	Canonical variate 3
Climate			
Aridity index	0.97	−0.01	−0.23
PREC	0.89	0.45	0.08
TEMP	−0.16	0.98	−0.09
Skull morphology			
ABL	−0.78	−0.26	−0.04
AIL	0.62	0.08	−0.31
AJL	0.65	0.20	−0.18
AML	0.52	−0.13	−0.12
ASL	0.53	0.51	0.07
ASW	0.17	−0.25	−0.26
BH	−0.78	−0.20	−0.15
BO	0.50	0.06	−0.13
BW	−0.71	−0.30	−0.04
CB	0.56	0.28	0.10
DL	0.39	0.32	−0.26
ID	0.20	0.46	−0.15
IH	0.16	0.02	−0.29
IOB	−0.50	0.25	0.11
IW	0.72	−0.07	0.06
JDL	0.35	0.19	−0.18
JID	0.44	0.27	−0.25
JMH	0.13	−0.15	0.17
JML	0.51	−0.13	−0.02
JMW	−0.01	0.08	0.23
LIW	0.51	−0.10	0.15
MAM	0.26	0.24	−0.24
MB	0.77	0.16	−0.05
MH	−0.16	−0.08	0.26
MW	0.00	0.11	0.04
NB	0.63	−0.14	0.30
NSL	0.29	0.40	0.34
PR	0.29	0.47	0.05
RD	0.45	0.15	−0.35

structure and aridity has never been directly tested before. Kenagy (1972) was the first to propose that the broad, flat, and chisel-shaped lower incisors of *Dipodomys microps* was an adaptation to remove the salt-coated epidermis of halophytic plants that occur in their habitat before ingestion, a character and behavior that was thought to be unique among rodents. In a comparison of 7 species of desert rodents from several continents, Ojeda et al. (1999) showed that in addition to *D. microps*, *Tympanoctomys barrerae* and *Psammomys obesus* (from the Great Basin, Monte, and Sahara deserts, respectively) have evolved similar-shaped incisors and the ability to remove salt from desert saltbush epidermis before ingesting the green mesophyll tissue, with increased specialization being correlated with increased "squareness" of the lower incisors. Perhaps it is unsurprising that we did not find a correlation, since the sample of rodents display a very large range of dietary variation both within and between habitat groups

(e.g., Alhajeri and Steppan 2018), with many of the sampled desert rodents not being found in habitats that contain saltbush. An association may be observed if analyses were limited to folivorous species and excluded other dietary types such as granivorous species.

Both the NI and the NV scores were significantly positively correlated with mean annual precipitation or aridity index scores, indicating that more arid environments are correlated with longer and narrower nasals and smaller NVs. If the NI and NV measures approximate turbinate morphology, then the results are consistent with the expectation of desert adaptation in rodents, where long, narrow, and extremely convoluted turbinates are the most effective at conserving water from exhaled air (Schmidt-Nielsen and Schmidt-Nielsen 1950; Cortes et al. 1988, 1990; Feldhamer et al. 2007).

One of the most important functions of the nasal cavity is to moisten and warm inhaled air to prevent damage of sensitive

mucosal lung tissues and to cool and dry exhaled air, facilitating water retention (Inthavong et al. 2007; Noback et al. 2011). Water and heat exchange between air and mucosal tissue are more efficient in longer and narrower turbinate systems due to increased mucosal contact surface per unit volume of inhaled air, because both the surface to volume ratio of the nasal passages and the resistance time (time air is spends in the nasal cavity) are increased (Inthavong et al. 2007). This relationship is also seen across human populations (Leong and Eccles 2009; Noback et al. 2011).

The association of the NI (the ratio between nasal breadth and length) with aridity was weaker than for NV, which could reflect an adaptive trade-off or constraint with fossoriality (which is not expected to be reflected in the rostral height) because most small desert rodents avoid heat stress by burrowing (e.g., gerbils, kangaroo rats, and dipodids—Nowak 1999), where long, projecting nasals hinder digging efficiency and have a greater chance of injury (Agrawal 1967). Many desert animals have also evolved a counter-current heat exchange system in their nasal passages to further enhance water retention (Schmidt-Nielsen 1972), a structure that is not adequately captured by cranial measurements.

Desert adaption in overall skull morphology.—Desert and mesic species have extensive overlap in overall skull morphology. However, the multivariate association between overall morphology and climate was significant, exhibiting strong correlations between some morphological traits with climatic variables. The strongest association was between increased auditory bulla dimensions (length, height, and width), reduced basicranial width and reduced (upper) incisor breadth, and more arid environments. Other linear measurements, including the components in the calculation of the LII and the NI or volume, were much more weakly correlated with aridity than those in bullar dimensions. Phylogenetically corrected analyses do not support associations between other traits and habitat or aridity measures. Other than the upper incisor width, dental characters were not associated with aridity despite many examples of dietary specialization in desert rodents. Desert rodents have different specializations ranging from exclusively folivorous (some with the capacity to shave and consume halophytic plants) to exclusively granivorous, and it is likely that only the former are associated with "squarer" incisors (e.g., Ojeda et al. 1999).

Conclusions.—Rodents transitioned very frequently between desert and mesic habitats throughout their evolutionary history, indicating flexible habitat choice and frequent habitat switches. Despite this pattern, there is a bias towards a transition from a mesic to a desert habitat. Some traits long considered to be adaptations to desert conditions appear to have arisen within several clades (gerbils, heteromyids, and dipodids) after they had already begun diversifying within desert habitats, not coincident with the transition to deserts. Previously recognized associations between morphology and deserts were inflated due to shared phylogenetic history. Nonetheless, we confirm prior hypotheses that auditory bullae enlarged significantly with increased aridity, and this was the strongest morphological association we found (Figs. 3 and 7; Supplementary Data SD17). The discordance between the strong pattern observed

in the plots, when compared with the low R^2 values (Fig. 3; Supplementary Data SD17), may partly be attributed to the overly conservative nature of phylogenetic corrections, especially when related species share both habitat and traits due to stabilizing selection. For example, many species in arid environments may share large bullae because they are related to each other. Alternatively, the low R^2 values may also indicate that the relationship is weak at the order level, when compared to narrower taxonomic scales.

We also confirm a significant positive correlation between increased lengthening and narrowing of the nasals, and reduced NV, with increased aridity, wherein lengthened, narrowed, and convoluted nasal passages are more efficient at conserving water from exhaled air. Incisor shape was not significantly associated with habitat or climate, perhaps due to different responses to dietary selective pressures in different deserts. Desert and mesic rodents overlap extensively in the morphospace represented by other skull characters indicating no significant difference between desert and mesic species in overall skull morphology or in traits not previously proposed as desert or arid adaptations.

SUPPLEMENTARY DATA

Supplementary data are available at *Journal of Mammalogy* online.

Supplementary Data SD1.—List of all extant rodent species listed in IUCN grouped into desert, mesic, or unknown habitat categories.

Supplementary Data SD2.—Average of the raw bioclimatic variables encountered by species within their range. Variables and units are described in Supplementary Data SD3.

Supplementary Data SD3.—Description and units of the bioclimatic variables from Supplementary Data SD2.

Supplementary Data SD4.—Species means of raw distances extracted from the ventral views of crania in millimeters. Taxa sorted taxonomically, and a visual representation of distances can be found in the figures below. # = number of specimens used. BL = total length of the auditory bulla; BO = basioccipital length; BW = bulla width; CB = condyle breadth; DL = diastema length; IW = incisor width; MB = basicranial width; ML = molar tooth row length; MW = 1st molar width; PR = pterygoid region length; SL = skull length; SW = skull width.

Supplementary Data SD5.—Visual depictions of linear distances extracted from the ventral views of crania as described in Supplementary Data SD4. Distances are displayed on the cranium of the western jumping mouse (*Zapus princeps*; AMNH 124327).

Supplementary Data SD6.—Species means of raw distances extracted from the lateral and dorsal views of crania in millimeters. See Supplementary Data SD4 legend for more information. BH = bulla height across auditory meatus and perpendicular to LBL; DSL = dorsal skull length; DSW = dorsal skull width; ID = incisor depth; IH = incisor height; IOB = interorbital breadth; MH = 1st molar height (hypsodonty measurement); LBL = maximum lateral bulla length; LML = lateral

molar row length; NB = nasal breadth; NSL = nasal length; RD = rostral depth.

Supplementary Data SD7.—Visual depictions of linear distances extracted from the lateral views of crania as described in Supplementary Data SD6. Distances are displayed on the cranium of the common cane mouse (*Zygodontomys brevicauda*; MVZ 113383).

Supplementary Data SD8.—Visual depictions of linear distances extracted from the dorsal views of crania as described in Supplementary Data SD6. Distances are displayed on the cranium of Spegazzini's grass mouse (*Akodon spegazzinii*; UF 27623).

Supplementary Data SD9.—Species means of raw distances extracted from the occlusal and lateral views of mandibles in millimeters. See Supplementary Data SD4 legend for more information. IL = incisor length (occlusal mandible view); IL2 = incisor length (lateral mandible view); JDL = jaw diastema length; JID = jaw incisor depth; JLB = jaw length measurement II; JLS = jaw length measurement I; JMH = jaw 1st molar height; JML = jaw molar tooth row length; JMW = jaw 1st molar width; LIW = width across both lower incisors; MAM = moment arm masseter; TJL = total jaw length.

Supplementary Data SD10.—Visual depictions of linear distances extracted from the occlusal views of mandibles as described in Supplementary Data SD9. Distances are displayed on the mandible of the Texas antelope squirrel (*Ammospermophilus interpres*; USNM 18154).

Supplementary Data SD11.—Visual depictions of linear distances extracted from the lateral views of mandibles as described in Supplementary Data SD9. Distances are displayed on the mandible of the big-eared climbing rat (*Ototylomys phyllotis*; FMNH 64565).

Supplementary Data SD12.—Species means of characters derived from raw distances described above. See Supplementary Data SD4 legend for more information. ABL = average bulla length; AIL = average incisor length; AJL = average jaw length; AML = average molar length; ASL = average skull length; ASW = average skull width; BI = bulla index; BV = bulla volume; LII = lower incisor index; NI = nasal index; NV = nasal volume.

Supplementary Data SD13.—Summarized composite chronogram of 591 rodent OTUs with collected morphological data. Molecular phylogeny modified from Fabre et al. (2012) and Steppan and Schenk (2017). Major taxonomic groups are indicated. Red tips indicate desert species, black tips indicate mesic species, and blue tips indicate species with ambiguous habitat; black branches do not signify habitat. Figure provided for illustrative purposes and was used for ancestral state reconstruction (full 2,414 OTU trees used). Species labels are in Supplementary Data SD14 and trees summarizing results of ancestral state reconstruction are in Supplementary Data SD15 and SD16.

Supplementary Data SD14.—Composite chronogram of 591 rodent OTUs with collected morphological data. Molecular phylogeny modified from Fabre et al. (2012) and Steppan and Schenk (2017). Some of the major taxonomic groups are indicated.

Supplementary Data SD15.—Maximum likelihood ancestral state reconstruction of habitat in 2,277 species of extant rodents. Red tips and nodes indicate desert species and green tips and nodes indicate mesic species based on IUCN habitat information for the tips.

Supplementary Data SD16.—One of 1,000 stochastic character maps used for ancestral character state estimation in the BI framework. See Supplementary Data SD15 legend for more information.

Supplementary Data SD17.—Association between bulla volume scores with (a) habitat, (b) aridity index, (c) mean annual precipitation, and (d) mean annual temperature. See Fig. 3 legend for information.

Supplementary Data SD18.—Association between lower incisor index scores with (a) habitat, (b) aridity index, (c) mean annual precipitation, and (d) mean annual temperature. See Fig. 3 legend for information.

Supplementary Data SD19.—Variation in desert and mesic rodents in the first 6 phylogenetic principal component morphospace of the 29 desert-neutral cranial characters. Principal components 1–6 explain 19.6, 12.0, 10.5, 9.6, 8.0, and 5.7% of the variation, respectively.

Supplementary Data SD20.—The first 6 phylogenetic principal component loadings of the 29 desert-neutral characters indicating the relative contribution of each morphological character.

Supplementary Data SD21.—Variation in desert and mesic rodents in the morphospace represented by the sole discriminant function of the 29 desert-neutral cranial characters.

Supplementary Data SD22.—Discriminant function coefficients of the 29 desert-neutral cranial characters indicating the relative contribution of each morphological character.

Supplementary Data SD23.—Proportion of correct habitat classifications based on the linear discriminant function of the 29 desert-neutral characters using both the original data and cross-validated data based on jackknife resampling. Observed and predicted habitat categories are indicated in the rows and columns, respectively.

LITERATURE CITED

AGRAWAL, V. C. 1967. Skull adaptations in fossorial rodents. Mammalia 31:300–312.

ALHAJERI, B. H., O. J. HUNT, AND S. J. STEPPAN. 2015. Molecular systematics of gerbils and deomyines (Rodentia: Gerbillinae, Deomyinae) and a test of desert adaptation in the tympanic bulla. Journal of Zoological Systematics and Evolutionary Research 53:312–330.

ALHAJERI, B. H., AND S. J. STEPPAN. 2016. Association between climate and body size in rodents: a phylogenetic test of Bergmann's rule. Mammalian Biology - Zeitschrift für Säugetierkunde 81:219–225.

ALHAJERI, B. H., AND S. J. STEPPAN. 2018. Ecological and ecomorphological specialization are not associated with diversification rates in muroid rodents (Rodentia: Muroidea). Evolutionary Biology 1–19. doi:10.1007/s11692-018-9449-8

BALTAS, E. 2007. Spatial distribution of climatic indices in northern Greece. Meteorological Applications 14:69–78.

BLOMBERG, S. P., T. J. GARLAND, AND A. R. IVES. 2003. Testing for phylogenetic signal in comparative data: behavioral traits are more labile. Evolution 57:717–745.

BOLLBACK, J. P. 2006. SIMMAP: stochastic character mapping of discrete traits on phylogenies. BMC Bioinformatics 7:88.

BORATYŃSKI, Z., ET AL. 2017. Repeated evolution of camouflage in speciose desert rodents. Scientific Reports 7:3522.

BURDA, H., V. BRUNS, AND E. NEVO. 1989. Middle ear and cochlear receptors in the subterranean mole-rat, *Spalax ehrenbergi*. Hearing Research 39:225–230.

BUTTS, C. 2012. Yacca: Yet Another Canonical Correlation Analysis Package. R package version 1.1. http://CRAN.R-project.org/package=yacca/.

CARLETON, M. D., AND G. G. MUSSER. 2005. Order Rodentia. Pp. 745–752 in Mammal species of the world, Third Edition (D. E. Wilson and D. M. Reeder, eds.). The Johns Hopkins University Press, Baltimore, Maryland.

CORTES, A., M. ROSENMANN, AND C. BÁEZ. 1990. Función del riñón y del pasaje nasal en la conservación de agua corporal en roedores simpátridos de Chile central. Revista Chilena de Historia Natural 63:279–291.

CORTES, A., C. ZULETA, AND M. ROSENMANN. 1988. Comparative water economy of sympatric rodents in a Chilean semi-arid habitat. Comparative Biochemistry and Physiology 91A 9:711–714.

DE MARTONNE, E. 1927. Regions of interior basin drainage. Geographical Review 17:397–414.

DE MARTONNE, E. 1942. Nouvelle carte mondiale de l'indice d'aridité. Annales de Géographie 51:242–250.

FABRE, P. H., L. HAUTIER, D. DIMITROV, AND E. P. DOUZERY. 2012. A glimpse on the pattern of rodent diversification: a phylogenetic approach. BMC Evolutionary Biology 12:1–19.

FELDHAMER, G. A., L. C. DRICKAMER, S. H. VESSEY, J. F. MERRITT, AND C. KRAJEWSKI. 2007. Mammalogy: adaptation, diversity, ecology. JHU Press, Baltimore, Maryland.

FRANCESCOLI, G. 1999. A preliminary report on the acoustic communication in Uruguayan *Ctenomys* (Rodentia, Octodontidae): basic sound types. Bioacoustics 10:203–218.

FRANCESCOLI, G. 2000. Sensory capabilities and communication in subterranean rodents. Pp. 111–144 in Life underground: the biology of subterranean rodents (E. A. Lacey, J. L. Patton, and G. N. Cameron, eds.). University of Chicago Press, Chicago, Illinois.

FRANCESCOLI, G., V. QUIRICI, AND R. SOBRERO. 2012. Patterns of variation in the tympanic bulla of tuco-tucos (Rodentia, Ctenomyidae, *Ctenomys*). Acta Theriologica 57:153–163.

FRECKLETON, R. P., P. H. HARVEY, AND M. PAGEL. 2002. Phylogenetic analysis and comparative data: a test and review of evidence. The American Naturalist 160:712–726.

GARDNER, A., AND L. EMMONS. 1984. Species groups in *Proechimys* (Rodentia, Echimyidae) as indicated by karyology and bullar morphology. Journal of Mammalogy 65:10–25.

GARLAND, T., A. W. DICKERMAN, C. M. JANIS, AND J. A. JONES. 1993. Phylogenetic analysis of covariance by computer simulation. Systematic Biology 42:265–292.

GONZÁLEZ, I., S. DÉJEAN, P. MARTIN, AND A. BACCINI. 2008. CCA: an R package to extend canonical correlation analysis. Journal of Statistical Software 23:1–14.

HÄRDLE, W., AND L. SIMAR. 2012. Applied multivariate statistical analysis. 3rd ed. Springer, New York.

HARMON, L. J., J. T. WEIR, C. D. BROCK, R. E. GLOR, AND W. CHALLENGER. 2008. GEIGER: investigating evolutionary radiations. Bioinformatics 24:129–131.

HEFFNER, R. S., AND H. HEFFNER. 1992. Hearing and sound localization in blind mole rats: *Spalax ehrenbergi*. Hearing Research 62:206–216.

HICKMAN, C. P., L. S. ROBERTS, A. LARSON, AND H. I'ANSON. 2004. The biosphere and animal distribution. Pp. 806–823 in Integrated principles of zoology (P. E. Reidy and D. A. Henricks, eds.). 12th ed. McGraw-Hill College, Boston, Massachusetts.

HIJMANS, R. J., S. E. CAMERON, J. L. PARRA, P. G. JONES, AND A. JARVIS. 2005. Very high resolution interpolated climate surfaces for global land areas. International Journal of Climatology 25:1965–1978.

HIJMANS, R. J., L. GUARINO, AND P. MATHUR. 2012. DIVA-GIS version 7.5. A geographic information system for the analysis of species distribution data. http://www.diva-gis.org/.

HUANG, G., J. ROSOWSKI, M. RAVICZ, AND W. PEAKE. 2002. Mammalian ear specializations in arid habitats: structural and functional evidence from sand cat (*Felis margarita*). Journal of Comparative Physiology A 188:663–681.

HUELSENBECK, J. P., R. NIELSEN, AND J. P. BOLLBACK. 2003. Stochastic mapping of morphological characters. Systematic Biology 52:131–158.

INTHAVONG, K., Z. F. TIAN, AND J. Y. TU. 2007. CFD simulations on the heating capability in a human nasal cavity. Pp. 842–847 in Proceedings of the 16th Australasian Fluid Mechanics Conference.

IUCN. 2013. IUCN Red List of Threatened Species. Version 2013.1. http//www.iucnredlist.org/. Accessed 26 August 2013.

KENAGY, G. J. 1972. Saltbush leaves: excision of hypersaline tissue by a kangaroo rat. Science 178:1094–1096.

LAY, D. M. 1972. The anatomy, physiology, functional significance and evolution of specialized hearing organs of Gerbillinae rodents. Journal of Morphology 138:41–120.

LEONG, S. C., AND R. ECCLES. 2009. A systematic review of the nasal index and the significance of the shape and size of the nose in rhinology. Clinical Otolaryngology 34:191–198.

LOUW, G., AND M. SEELY. 1982. Ecology of desert organisms. Longman, London, United Kingdom.

LUNGU, M., L. PANAITESCU, AND S. NI . 2011. Aridity, climatic risk phenomenon in Dobrudja. Present Environment and Sustainable Development 5:179–190.

MALIVA, R., AND T. MISSIMER. 2012. Chapter 2: aridity and drought. Pp. 21–39 in Arid lands water evaluation and management. Springer Berlin/Heidelberg, New York.

MARES, M. A. 1975. South American mammal zoogeography : evidence from convergent evolution in desert rodents. Proceedings of the National Academy of Science USA 72:1702–1706.

Mares, M. A. 1976. Convergent evolution of desert rodents: multivariate analysis and zoogeographic implications. Paleobiology 2:39–63.

Mason, M. J. 2001. Middle ear structures in fossorial mammals: a comparison with non-fossorial species. Journal of Zoology 255:467–486.

Mason, M. J. 2003. Morphology of the middle ear of golden moles (Chrysochloridae). Journal of Zoology 260:391–403.

Mason, M. J. 2015. Structure and function of the mammalian middle ear. I: large middle ears in small desert mammals. Journal of Anatomy 228:284–299.

McCoy, M., B. Bolker, C. Osenberg, B. Miner, and J. Vonesh. 2006. Size correction: comparing morphological traits among populations and environments. Oecologia 148:547–554.

Momtazi, F., J. Darvish, F. Ghassemzadeh, and A. Moghimi. 2008. Elliptic Fourier analysis on the tympanic bullae in three *Meriones* species (Rodentia, Mammalia): its application in biosystematics. Acta Zoologica Cracoviensia, Series A: Vertebrata 51:49–58.

Mundry, R. 2014. Statistical issues and assumptions of phylogenetic generalized least squares. Pp. 1–552 in Modern phylogenetic comparative methods and their application in evolutionary biology (L. Z. Garamszegi, eds.). Springer-Verlag Berlin Heidelberg.

Ndiaye, A., et al. 2012. Evolutionary systematics and biogeography of endemic gerbils (Rodentia, Muridae) from Morocco: an integrative approach. Zoologica Scripta 41:11–28.

Noback, M. L., K. Harvati, and F. Spoor. 2011. Climate-related variation of the human nasal cavity. American Journal of Physical Anthropology 145:599–614.

Nowak, R. M. 1999. Walker's mammals of the world. 6th ed. John Hopkins University Press, Baltimore, Maryland. Vol. 1 and 2.

Ojeda, R. A., C. E. Borghi, G. B. Diaz, S. M. Giannoni, M. A. Mares, and J. K. Braun. 1999. Evolutionary convergence of the highly adapted desert rodent *Tympanoctomys barrerae* (Octodontidae). Journal of Arid Environments 41:443–452.

Orme, D., et al. 2013. CAPER: Comparative Analyses of Phylogenetics and Evolution in R. R package version 0.5.2. http://cran.r-project.org/web/packages/caper/.

Paradis, E., J. Claude, and K. Strimmer. 2004. APE: Analyses of Phylogenetics and Evolution in R language. Bioinformatics 20:289–290.

Pavlinov, I. Y., and K. A. Rogovin. 2000. Relation between size of pinna and of auditory bulla in specialized desert rodents. Journal of General Biology 61:87–101.

R Development Core Team. 2013. R: a language and environment for statistical computing. R Foundation for Statistical Computing, Vienna, Austria. http://www.r-project.org/.

Randall, J. A. 1993. Behavioural adaptations of desert rodents (Heteromyidae). Animal Behaviour 45:263–287.

Revell, L. J. 2009. Size-correction and principal components for interspecific comparative studies. Evolution 63:3258–3268.

Revell, L. J. 2012. Phytools: an R package for phylogenetic comparative biology (and other things). Methods in Ecology and Evolution 3:217–223.

Robertson, R. A., and A. R. Shadle. 1954. Osteologic criteria of age in beavers. Journal of Mammalogy 35:197–203.

Rohlf, F. J. 2010. TpsDig. Version 2.16. Department of Ecology and Evolution, State University of New York, Stony Brook.

Samuels, J. X. 2009. Cranial morphology and dietary habits of rodents. Zoological Journal of the Linnean Society 156:864–888.

Schleich, C. E., and A. I. Vasallo. 2003. Bullar volume in subterranean and surface-dwelling caviomorph rodents. Journal of Mammalogy 84:185–189.

Schmidt-Nielsen, K. 1972. How animals work. Cambridge University Press, Cambridge, England.

Schmidt-Nielsen, B., and K. Schmidt-Nielsen. 1950. Pulmonary water loss in desert rodents. American Journal of Physiology 162:31–36.

Shenbrot, G. I., B. R. Krasnov, and K. A. Rogovin. 1999. Spatial ecology of desert rodent communities. Springer-Verlag Berlin Heidelberg, New York.

Sowell, J. 2001. Desert ecology: an introduction to life in the arid southwest. University of Utah Press, Salt Lake City, Utah.

Squarcia, S. M., N. S. Sidorkewicj, and E. B. Casanave. 2007. The hypertrophy of the tympanic bulla in three species of dasypodids (Mammalia, Xenarthra) from Argentina. International Journal of Morphology 25:597–602.

Stacklies, W., H. Redestig, M. Scholz, D. Walther, and J. Selbig. 2007. PcaMethods—a bioconductor package providing PCA methods for incomplete data. Bioinformatics 23:1164–1167.

Steppan, S. J. 1997. Phylogenetic analysis of phenotypic covariance structure. I. contrasting results from matrix correlation and common principal component analysis. Evolution 51:571–586.

Steppan, S. J., and J. J. Schenk. 2017. Muroid rodent phylogenetics: 900-species tree reveals increasing diversification rates. PLoS ONE 12:1–31.

UCLA: Statistical Consulting Group. 2013. Introduction to SAS. http://www.ats.ucla.edu/stat/sas/notes2/. Accessed 10 November 2013.

Venables, W. N., and B. D. Ripley. 2002. Modern applied statistics with S. 4th ed. Springer, New York.

Verzi, D. H., and A. I. Olivares. 2006. Craniomandibular joint in South American burrowing rodents (Ctenomyidae): adaptations and constraints related to a specialized mandibular position in digging. Journal of Zoology 270:488–501.

Vial, J. L. 1962. The auditory bulla of *Dipodomys deserti* (Rodentia) and evidence of its adaptive significance. Revista de Biología Tropical 10:11–18.

Wainwright, P. C., and S. M. Reilly. 1994. Ecological morphology: integrative organismal biology. University of Chicago Press, Chicago, Illinois.

Ward, D. 2009. The biology of deserts. Oxford University Press, Oxford, United Kingdom.

Webster, D., and M. Webster. 1975. Auditory systems of Heteromyidae: functional morphology and evolution of the middle ear. Journal of Morphology 146:343–376.

Appendix I

Specimens examined.—The specimens examined are listed by the following acronyms: American Museum of Natural History (AMNH), Field Museum of Natural History (FMNH), Museum of Vertebrate Zoology (MVZ), United States National Museum of Natural History (USNM), the University of Florida Museum of Natural History (FLMNH), Laboratorio de Citogenetica Mamiferos, Universidad de Chile (LCM), Oklahoma Museum of Natural History (OMNH).

Anomaluromorpha.—Pedetidae: *Pedetes capensis* USNM 422522; FMNH 38263, 38231, 38261.

Castorimorpha.—Geomyidae: *Cratogeomys castanops* AMNH 68767, 68766, 68768, 63812. *Thomomys umbrinus* USNM 55913; FLMNH 8238; FMNH 14058, 14059. Heteromyidae: Dipodomyinae: *Dipodomys agilis* USNM 192339; FLMNH 432, 3057, 3056. *Dipodomys californicus* USNM 36389, 23545, 23543, 44152. *Dipodomys compactus* USNM 43537, 43308, 42871, 100058. *Dipodomys deserti* USNM 33926; AMNH 139598, 139597, 139600, 139599. *Dipodomys elator* USNM 348461, 348460, 348459, 101124. *Dipodomys gravipes* USNM 138910, 245885, 245884. *Dipodomys heermanni* USNM 149736. 137911, 137918, 149735. *Dipodomys ingens* USNM 128801, 214505, 128802, 214485. *Dipodomys merriami* USNM 50007; AMNH 173786, 169577, 173787. *Dipodomys microps* MVZ 73650, 73651, 73649, 73652. *Dipodomys nelsoni* MVZ 76548, 76547; USNM 56195, 51068. *Dipodomys nitratoides* USNM 54871, 149756, 214515, 149757. *Dipodomys ordii* USNM 214113; FLMNH 24179, 24180, 4673. *Dipodomys panamintinus* USNM 41336; FLMNH 3058, 3059, 3060. *Dipodomys phillipsii* USNM 53324, 53331, 90803, 94622. *Dipodomys simulans* USNM 555015, 555018, 139866, 531718. *Dipodomys spectabilis* USNM 46288; FLMNH 25951, 25952, 25953. *Dipodomys stephensi* USNM 150613, 118393, 94042, 94043. *Dipodomys venustus venustus* USNM 130113, 130114, 51847, 150940. *Dipodomys venustus elephantinus* USNM 150948, 67151, 69448, 150962. *Microdipodops megacephalus* MVZ 159877, 159878; USNM 54585, 54582. *Microdipodops pallidus* USNM 246133, 246023, 246020, 246024. Heteromyinae: *Heteromys anomalus* USNM 540709; FLMNH 13349, 13709, 23863. *Heteromys australis* USNM 310391, 310402, 310393, 310394. *Heteromys catopterius* USNM 517545, 370977, 405985, 517566. *Heteromys d. desmarestianus* USNM 391895; FLMNH 6822, 6823, 6824. *Heteromys d. goldmani* USNM 275249, 275233, 275242, 77581. *Heteromys gaumeri* USNM 108480, 108481, 108479, 108131. *Heteromys nelsoni* USNM 77578; FMNH 41759, 41761, 41760. *Heteromys oasicus* USNM 456324, 456327. *Heteromys teleus* USNM 528573. *Liomys adspersus* USNM 323676, 323674, 296299, 323672. *Liomys irroratus* USNM 120169; FLMNH 6202, 6203, 6206. *Liomys pictus* USNM 126914; FLMNH 6168, 6173, 6171. *Liomys salvini* USNM 275285; FLMNH 6161, 6164, 6165. Perognathinae: *Chaetodipus arenarius* USNM 531519, 531529, 146908, 531518. *Chaetodipus artus* USNM 96303, 96304, 96301, 96302. *Chaetodipus baileyi* USNM 49169; FLMNH 3076; FMNH 52836, 52839. *Chaetodipus californicus* USNM 55561; FLMNH 3033; FMNH 10902, 10890. *Chaetodipus eremicus* USNM 51096, 157404, 119104, 119781. *Chaetodipus fallax* USNM 529907; FLMNH 3044, 12761, 12760. *Chaetodipus formosus* USNM 262926, 263160, 41957, 263139; AMNH 11850, 11837, 258740, 258738. *Chaetodipus goldmani* USNM 96325, 96672, 96328, 96674. *Chaetodipus hispidus* USNM 31559; FLMNH 9633, 11944, 8672. *Chaetodipus intermedius* USNM 532532; FLMNH 12527, 12528, 7836. *Chaetodipus lineatus* USNM 296791, 296790; FMNH 141795, 141796. *Chaetodipus nelsoni* USNM 50210; FMNH 46911, 46910. *Chaetodipus penicillatus* USNM 552796; FLMNH 4681, 437, 4682. *Chaetodipus pernix* USNM 96679, 96681, 95822, 96327. *Chaetodipus rudinoris* USNM 145985, 146090, 14005, 140006. *Chaetodipus spinatus* USNM 140038; FLMNH 3041, 3042, 3043. *Perognathus alticolus* USNM 91561, 127813, 91562, 127811. *Perognathus amplus* MVZ 47107, 47108, 47109, 47110. *Perognathus fasciatus* USNM 168602, 179713, 202337, 179714. *Perognathus flavescens* USNM 47378, 87901, 66537, 275699. *Perognathus flavus* USNM 213440; FLMNH 7833, 7834, 24183. *Perognathus inornatus* USNM 41789, 93726, 41788, 149800. *Perognathus longimembris* MVZ 55750, 60834, 55751, 55752. *Perognathus merriami* USNM 48743, 48741, 93349, 48742. *Perognathus parvus* USNM 55294; FMNH 11886, 11887, 11889.

Hystricomorpha.—Abrocomidae: *Abrocoma bennettii* USNM 391842; FLMNH 23915; FMNH 23170, 23169. Bathyergidae: *Bathyergus janetta* USNM 469790, 469794, 469791, 469793. *Cryptomys hottentotus* USNM 221431, 344826, 344869, 221431. Caviidae: Caviinae: *Microcavia australis* USNM 84182; FLMNH 27628, 27636, 27645. Dolichotinae: *Dolichotis patagonum* USNM 135946; FLMNH 9949, 18999; FMNH 49212. *Dolichotis salinicola* USNM 258569, 270234, 257010, 270306. Chinchillidae: *Lagidium viscacia* USNM 274565; FLMNH 23901; FMNH 53673, 53672. *Lagostomus maximus* USNM 114840; FLMNH 14778; FMNH 54339, 53704. Ctenodactylidae: *Ctenodactylus gundi* MVZ 201015; USNM 475997, 475998, 476005. *Ctenodactylus vali* USNM 302296. *Felovia vae* USNM 401279, 401286, 402149, 402147. *Massoutiera mzabi* USNM 482508, 482509, 482510; FMNH 48806. *Pectinator spekei* FMNH 106442, 1438. Ctenomyidae: *Ctenomys emilianus* FMNH 29064. *Ctenomys latro* USNM 236335, 236336; FMNH 29058, 41270. *Ctenomys mendocinus* FMNH 46131, 46130, 46132, 46133. *Ctenomys occultus* FMNH 41267, 41268. Hystricidae: *Hystrix africaeaustralis* USNM 368422, 469825, 221369, 470121. *Hystrix cristata* USNM 162900; FMNH 57170, 89203, 41337. *Hystrix indica* USNM 327158, 350765, 522678, 350763. Octodontidae: *Octodon degus* USNM 541816, 259581; FLMNH 14997, 14998. *Octodon lunatus* FLMNH 23916; FMNH 23210, 23203, 23903. Petromuridae: *Petromus typicus* MVZ 117767; USNM 343968, 343962, 343963.

Myodonta.—Dipodoidea: Dipodidae: Allactaginae: *Allactaga balikunica* FMNH 123651. *Allactaga bullata* AMNH 58522, 58773, 84202, 46403. *Allactaga elater* MVZ 192029; USNM 369890, 341604, 369889; AMNH 88749; FMNH 103865, 103867, 103868. *Allactaga euphratica* USNM 327719, 327721, 327723, 327722. *Allactaga firouzi* FMNH 112350, 112349, 112351.

Allactaga hotsoni MVZ 192030, 192031, 192034, 192033. *Allactaga major* USNM 251639, 1445, 254957; AMNH 178795. *Allactaga severtzovi* AMNH 206589, 176269. *Allactaga sibirica* USNM 155186, 155187, 155194, 155190. *Allactaga tetradactyla* USNM 317092, 317093, 317088, 317089. *Allactaga williamsi* USNM 327723, 327722; FMNH 82186, 82182. *Pygeretmus platyurus* USNM 547939. *Pygeretmus pumilio* USNM 1970, 1446, 192467, 122105. *Pygeretmus zhitkovi* AMNH 98133, 174330, 176264.

Cardiocraniinae: *Cardiocranius paradoxus* USNM 199550; AMNH 84154. *Salpingotulus michaelis* FMNH 99428, 106613. *Salpingotus crassicauda* USNM 547940; FMNH 137435. Dipodinae: *Dipus sagitta* USNM 155096, 544449, 155095, 573127; AMNH 84135, 58608, 84121, 58623. *Eremodipus lichtensteinii* AMNH 174329. *Jaculus blanfordi* MVZ 192035, 192036, 198826; USNM 354840, 354836. *Jaculus jaculus* MVZ 34198, 107727, 34199, 34200. *Jaculus orientalis* MVZ 32810, 183997; USNM 302289, 302290. *Paradipus ctenodactylus* AMNH 174332. *Stylodipus telum* MVZ 135291; USNM 547938, 4226; AMNH 174328. Sicistinae: *Sicista betulina* USNM 257391, 254986; AMNH 178814, 206586. *Sicista concolor* USNM 173798, 173797; AMNH 37837; FLMNH 26942, 26941. *Sicista napaea* AMNH 206587. *Sicista subtilis* USNM 122117, 122119; AMNH 178829, 206588. Zapodinae: *Eozapus setchuanus* USNM 240900, 240762; AMNH 113580; FMNH 36068. *Napaeozapus insignis* MVZ 101049, 96835, 96883, 96887. *Zapus hudsonius* MVZ 96834, 96880, 96881, 167703. *Zapus princeps* MVZ 84023, 84024, 84026, 84028; AMNH 124327; FLMNH 12734, 12741, 12731. *Zapus trinotatus* MVZ 99663, 99665, 99667, 99691. Muroidea: Calomyscidae: Calomyscinae: *Calomyscus baluchi* FLMNH 28486, 28503, 28504, 28502. *Calomyscus bailwardi* USNM 350196, 350198, 329048, 350200. Cricetidae: Arvicolinae: *Alticola strelzowi* AMNH 178819; FMNH 34034; USNM 175208, 175222, 175199, 175200. *Arvicola amphibius* FMNH 112222, 112223, 112224; FLMNH 22400. *Chionomys nivalis* MVZ 198808; USNM 369657, 104527, 105816. *Dicrostonyx groenlandicus* FLMNH 24163, 24407, 24167, 24116. *Ellobius talpinus* MVZ 41292, 41294, 41291, 135298. *Eolagurus luteus* AMNH 257136, 257135; FMNH 33720, 33721, 33722. *Eolagurus przewalskii* USNM 547936; FMNH 33720, 33721, 33722. *Eothenomys custos* AMNH 44140, 44150, 44156, 44147. *Lagurus lagurus* AMNH 87095, 176250, 176249, 257134. *Lasiopodomys mandarinus* AMNH 25438, 45439; USNM 172586, 299098. *Lemmus sibiricus* MVZ 128863, 128857, 128855, 128854. *Microtus arvalis* FMNH 103131, 103132, 103133; USNM 85655. *Microtus californicus* FMNH 10743, 10745, 10750; USNM 41607. *Microtus chrotorrhinus* AMNH 147362; MVZ 54425, 54427, 54426. *Microtus kikuchii* USNM 358625, 332965, 332967, 332964. *Microtus montanus* FMNH 12653, 12649, 12664; FLMNH 12732. *Microtus pennsylvanicus* FLMNH 3887, 3888, 3911; USNM 150132. *Microtus richardsoni* USNM 81384. *Myodes gapperi* MVZ 56815, 56816, 56813, 56814. *Neodon irene* USNM 449167, 449168, 449172, 449173. *Neofiber alleni* FLMNH 7418, 7421, 7445, 7440. *Ondatra zibethicus* FLMNH 1791, 1793, 1795, 2415. *Phenacomys intermedius* USNM 557668, 174477, 557669, 174432. *Prometheomys schaposchnikowi* AMNH 174334, 257138, 206579; USNM 547937. *Synaptomys cooperi* FLMNH 3839, 3841, 6436, 7946. Cricetinae: *Allocricetulus curtatus* USNM 259524. *Allocricetulus eversmanni* AMNH 176255, 59753; FMNH 33959, 33964; MVZ 41233; USNM 259524. *Cricetulus barabensis barabensis* MVZ 227428, 125072, 125071, 125068. *Cricetulus barabensis griseus* FMNH 33980, 33981, 33982, 33985. *Cricetulus longicaudatus*

MVZ 41235; USNM 172521, 576188, 449120. *Cricetulus migratorius* FLMNH 14594, 27124, 27145, 27142; MVZ 41234, 191941; USNM 326786, 326787. *Cricetus cricetus* AMNH 176483, 176484; MVZ, 41457, 129377. *Mesocricetus auratus* FMNH 63951; MVZ 102642, 102643; FLMNH 3987. *Phodopus campbelli* USNM 259901; FMNH 33973, 33974, 33978. *Phodopus roborovskii* USNM 155023, 155026, 155031, 155034. *Phodopus sungorus* AMNH 206570; MVZ 174380, 41239, 174379. Neotominae: *Habromys lepturus* USNM 68615, 68618, 68609, 68619. *Hodomys alleni* USNM 44633, 44634, 44626, 44627. *Isthmomys pirrensis* USNM 338302, 338269, 338306, 338270. *Megadontomys thomasi* MVZ 113564, 113558, 113559, 113562. *Neotoma albigula* USNM 212131; FLMNH 12618, 13245, 5386. *Neotoma bryanti* MVZ 186295, 195326, 186296, 186297. *Neotoma cinera* FLMNH 31327, 3166. *Neotoma devia* USNM 215546, 226400, 202463, 226399. *Neotoma floridana* FLMNH 14691, 12778, 166, 167. *Neotoma goldmani* MVZ 76946, 76947; USNM 116897, 116898. *Neotoma lepida* USNM 398296; FLMNH 458, 3164, 3163. *Neotoma mexicana* USNM 127314; FLMNH 6216, 7831, 5387. *Neotomodon alstoni* MVZ 91979, 91978, 91986, 91984. *Ochrotomys nutali* FLMNH 112, 12421, 2710, 801. *Onychomys leucogaster* FMNH 123451, 123450; FLMNH 24175, 12613, 941; USNM 273799. *Onychomys torridus* MVZ 72814, 119666, 28081, 28077. *Osgoodomys banderanus* USNM 45334, 45335, 45333, 33305. *Peromyscus aztecus* USNM 392010; FLMNH 24035, 24030, 24036. *Peromyscus boylii* FLMNH 6221, 6224, 6225, 6121; USNM 40514. *Peromyscus californicus* USNM 569214. *Peromyscus crinitus* USNM 53283; FLMNH 3078, 5394, 5397. *Peromyscus eremicus* FLMNH 9445, 9447, 9448; USNM 60100. *Peromyscus fraterculus* USNM 81017, 69556, 81016, 91566. *Peromyscus leucopus* FLMNH 9298, 9303, 1968; USNM 157114. *Peromyscus maniculatus* FLMNH 3637, 2802, 2803; USNM 530844. *Peromyscus merriami* MVZ 85828, 85836, 85832, 85831. *Peromyscus mexicanus* FLMNH 23931, 23930, 23929; USNM 314413. *Peromyscus pectoralis* MVZ 92138, 92135, 91786, 92140. *Peromyscus polionotus* FLMNH 13035, 5167, 786; USNM 308898. *Reithrodontomys creper* MVZ 164894, 164898, 164892, 164897. *Reithrodontomys fulvescens* FMNH 73418, 13115, 54147; USNM 70255. *Reithrodontomys gracilis* MVZ 98443, 98442; USNM 108143. *Reithrodontomys megalotis* FMNH 12273, 12271, 12270; FLMNH 6080, 6080, 6081, 6083; USNM 250559. *Scotinomys teguina* FMNH 128560, 128561; FLMNH 27717, 27712. *Xenomys nelsoni* USNM 45287, 45285. *Baiomys musculus* FMNH 54084, 54085, 54086; FLMNH 6039

Sigmodontinae: *Abrothrix andinus* MVZ 115690, 115691, 115689, 115697. *Abrothrix longipilis* MVZ 163783, 163784, 163782, 163783. *Aegialomys xanthaeolus* FMNH 194444, 19445; USNM 304528, 551641. *Akodon aerosus* FMNH 52529, 52524, 43232; USNM 507279. *Akodon boliviensis* FMNH 107917; MVZ 172907, 172953; FLMNH 9190. *Akodon iniscatus* MVZ 163790, 168995, 160118, 168996. *Akodon kofordi* MVZ 171660, 171662, 171661, 171663. *Akodon lutescens* USNM 259623. *Akodon mimus* MVZ 116109, 171748,

171751. *Akodon molinae* USNM 331060. *Akodon spegazzinii* FLMNH 27623, 27625, 27629, 27633. *Akodon torques* MVZ 171713, 171724, 174054; USNM 194638. *Andalgalomys pearsoni* FMNH 164184, 164188, 157341; MVZ 145278. *Andinomys edax* FMNH 162761; MVZ 120224, 120225, 141617. *Auliscomys sublimis* MVZ 139474, 139475, 115912, 139477. *Brucepattersonius igniventris* MVZ 191467, 183036, 191468, 183037. *Calomys callosus* FLMNH 27606, 27625, 27629, 27633; MVZ 145225, 145227, 145226, 145231. *Calomys lepidus* MVZ 115752, 174016, 116018, 115754. *Calomys musculinus* MVZ1 66067, 119954, 151015, 163390. *Calomys venustus* USNM 259264. *Cerradomys subflavus* MVZ 197609, 197542, 1970610, 197541. *Chelemys macronyx* MVZ 151013, 154583, 174384, 174382. *Chinchillula sahamae* MVZ 116034, 172675, 116181, 174023. *Delomys dorsalis* MVZ 183048, 183047, 183064, 183065. *Deltamys kempi* AMNH 206118, 206105, 206163, 206097. *Eligmodontia moreni* USNM 236312, 236313, 236311. *Eligmodontia morgani* MVZ 182663, 182665, 182675, 182668. *Eligmodontia typus* AMNH 262812; FMNH 124314, 124313, 124322; MVZ 169010. 174390, 174391; USNM 541732. *Euneomys chinchilloides* FMNH 50736, 134181; MVZ 186039, 186038. *Geoxus valdivianus* MVZ 162249, 159389, 154603, 154607. *Graomys edithae* MVZ 162261. *Graomys griseoflavus* FMNH 28423, 50920, 46125; MVZ 145252, 145254, 145255; FLMNH 27630; USNM 390214. *Holochilus brasiliensis* AMNH 210253; FMNH 136891, 87988, 88919. *Holochilus sciurus* FMNH 55476, 118813, 93050; FLMNH 13357. *Ichthyomys stolzmanni* AMNH 10109. *Irenomys tarsalis* MVZ 155837, 154620, 184955, 152171, 201154. *Juliomys pictipes* MVZ 182079, 197565, 197563, 197564. *Kunsia tomentosus* FMNH 122710, 122711; USNM 584515, 584516. *Lenoxus apicalis* MVZ 172657, 171511, 172656, 171513. *Loxodontomys micropus* MVZ 155836, 158475, 158474, 155827. *Melanomys caliginosus* MVZ 164873, 164871, 164870, 124057. *Microryzomys minutus* MVZ 115636, 171472, 173974, 166666. *Neacomys spinosus* MVZ 136626, 136629, 136625, 136627. *Necromys amoenus* MVZ 172884, 172886, 172881, 172885. *Nectomys apicalis* MVZ 153544, 153542, 153534, 153539. *Nectomys squamipes* FMNH 26741; FLMNH 6581, 6583, 30468. *Neotomys ebriosus* FMNH 75580; MVZ 114749, 114747, 172661. *Nephelomys keaysi* MVZ 173987, 171460, 171445, 171446. *Nephelomys livipes* FMNH 52703, 52702, 52705, 52708. *Notiomys edwardsii* MVZ 182132. *Oecomys bicolor* FMNH 117010, 116920, 116919; FLMNH 635. *Oecomys concolor* FMNH 87968; USNM 374321. *Oecomys superans* MVZ 155007, 200944, 153524, 155008. *Oligoryzomys fulvescens* FLMNH 6148, 28847, 6149, 6152. *Oligoryzomys longicaudatus* FLMNH 25933, 27622, 27671; USNM 259583. *Oligoryzomys microtis* FMNH 84349, 84350, 84351; USNM 584565. *Oryzomys couesi* FLMNH 9869, 29867, 29868, 6901. *Oryzomys palustris* FLMNH 23558, 23560, 23561; USNM 510842. *Oxymycterus hiska* AMNH 91602, 91601; MVZ 172660, 171520. *Oxymycterus nasutus* USNM 460550, 484395, 461881, 460551. *Phyllotis amicus* MVZ 136282, 136283, 115806, 137624, 138034, 145548. *Phyllotis andium* MVZ 135748, 135749, 135752, 135753. *Phyllotis caprinus* OMNH 30081, 30082. *Phyllotis darwini* LCM 3047, 3338, 4038, 4057, 4037, 4061. *Phyllotis gerbillus* MVZ 138024, 138028, 135693, 135695. *Phyllotis magister* MVZ 174036, 174038. *Phyllotis osilae* FMNH 52579, 107828, 107831; USNM 194576. *Phyllotis xanthopygus* LCM 3009, 3143, 3351, 3021. *Pseudoryzomys simplex* AMNH 262048; USNM 584585, 584586, 390668. *Punomys kofordi* MVZ 1147557, 114758, 116193. *Reithrodon auritus auritus* MVZ 163411, 172218, 171163, 165853. *Reithrodon auritus physodes* FLMNH 24357, 24358, 24359, 24360. *Rhagomys longilingua* FMNH 170687. *Rheomys thomasi* MVZ 98811, 98814, 98798, 98808. *Rhipidomys macconnelli* MVZ 160085, 160088, 160082, 160086. *Rhipidomys nitela* MVZ 197548, 197549, 197550, 197551. *Scapteromys tumidus* AMNH 235431; MVZ 183268, 183267, 183269. *Scolomys melanops* AMNH 67522. *Scolomys ucayalensis* MVZ 183166, 183169, 183167, 183168. *Sigmodon alstoni* FMNH 20040, 20042, 20045; USNM 442581. *Sigmodon arizonae* MVZ 62573, 62576, 62574, 62575. *Sigmodon fulviventer* MVZ 50867, 50866; USNM 20723, 247584. *Sigmodon hispidus* FLMNH 143, 1588, 1584, 1589. *Sigmodon ochrognathus* MVZ 80495, 80499, 80493, 80494. *Sigmodontomys alfari* FMNH 70536, 70535, 70534; MVZ 164891. *Sooretamys angouya ratticeps* FMNH 136919, 136920, 136922. *Thaptomys nigrita* FMNH 26820; MVZ 183043, 183040, 183044. *Thomasomys aureus* MVZ 166710, 166708, 166709, 166711. *Thomasomys daphne* AMNH 72128, 72112, 248283; FMNH 172378. *Thomasomys notatus* FMNH 170696; USNM 582122, 194898, 194897. *Transandinomys talamancae* FMNH 69207, 69211; MVZ 164879, 164878. *Wiedomys pyrrhorhinos* FMNH 136942; MVZ 197566, 197567. *Zygodontomys brevicauda* MVZ 106227, 113383; FLMNH 13359, 6574. Tylomyinae: *Nyctomys sumichrasti* MVZ 98817, 98818; FLMNH 7566, 7568, 7569, 7564. *Ototylomys phyllotis* FMNH 42043, 64564, 64567; FLMNH 6910. *Tylomys nudicaudus* FMNH 64569; MVZ 131365, 131364, 223323. Muridae: Deomyinae: *Acomys cahirinus* MVZ 107726, 118298, 118306, 1077262 118297, 1182982, 118320. *Acomys cineraceus* USNM 422402, 422404, 422401, 422419. *Acomys dimidiatus* MVZ 34193. *Acomys percivali* MVZ 186228, 186226, 186227, 186229. *Acomys ignitus* USNM 181744, 182888, 181750, 182889. *Acomys russatus* USNM 317002, 317007, 316997, 317006. *Acomys spinosissimus* AMNH 162547, 162546, 219041, 162545. *Acomys wilsoni* MVZ 186231, 186232, 186233, 191151. *Deomys ferrugineus* FMNH 167789, 167781, 167780; MVZ 196252. *Lophuromys flavopunctatus* USNM 259508, 537876, 259515, 537875. *Lophuromys zena* USNM 589948, 589952, 589943, 589947. *Lophuromys sikapusi* FMNH 81935, 81937, 81938; MVZ 196260. *Uranomys ruddi* USNM 438783, 367021, 438782, 367020. Gerbillinae: *Ammodillus imbellis* FMNH 140092. *Brachiones przewalskii* USNM 102578. *Desmodilliscus braueri* USNM 378287, 378289, 378290, 453904, 453899, 453893. *Desmodillus auricularis* MVZ 117381, 117379, 117371, 117372; AMNH 165455, 165453, 165451, 165456. *Dipodillus campestris* USNM 401028, 401038, 401036, 401852. *Dipodillus dasyurus* USNM 350041, 316662, 316658, 350037.

Dipodillus harwoodi USNM 162274, 162303, 162273, 162306. *Dipodillus lowei* USNM 297499, 297498. *Dipodillus mackilligini* USNM 316700. *Dipodillus maghrebi* USNM 472715, 472718, 472713, 472716, 472719, 472717. *Dipodillus simoni* USNM 316687, 316699, 316683, 350045. *Dipodillus stigmonyx* USNM 165286, 165283, 165284, 165285. *Gerbilliscus afra* MVZ 117338, 117337, 117340, 117342. *Gerbilliscus boehmi* USNM 162261, 162253, 162258, 162250. *Gerbilliscus brantsii brantsii* USNM 295355, 295350, 462447, 295349. *Gerbilliscus brantsii humpatensis* MVZ 88729, 88730. *Gerbilliscus brantsii perpallidus* AMNH 83696, 83693, 83694, 83695. *Gerbilliscus guineae* USNM 466209, 450763, 466212, 450765. *Gerbilliscus inclusus* USNM 538396, 538397, 538395, 381480. *Gerbilliscus kempi* MVZ 196265, 196266, 196267; FMNH 25369. *Gerbilliscus leucogaster* USNM 295398, 295400, 295394, 295395. *Gerbilliscus nigricaudus* USNM 183938, 590061, 183933, 590058. *Gerbilliscus phillipsi* USNM 344931, 344934; FMNH 28840, 28837. *Gerbilliscus robustus* MVZ 186208, 186207, 186204, 186205. *Gerbilliscus validus* MVZ 88727, 88732, 88717, 88720. *Gerbillurus paeba* AMNH 219001, 219002; MVZ 149573, 149576. *Gerbillurus setzeri* USNM 342232, 342260, 342229, 342233. *Gerbillurus tytonis* USNM 379852, 379869, 342165, 379854. *Gerbillurus vallinus* USNM 424171, 424172, 424173, 424175. *Gerbillus agag* MVZ 1543290, 154330, 154326, 154332. *Gerbillus amoenus* USNM 300231, 302217, 307626, 322544. *Gerbillus andersoni* MVZ 107721; USNM 316747, 283254, 300226. *Gerbillus aquilus* USNM 328042, 369319, 328045, 369341. *Gerbillus cheesmani* MVZ 191959, 191960; 29029, 29042. *Gerbillus famulus* USNM 321586, 321664, 321587, 321663. *Gerbillus floweri* USNM 316843, 316848, 316850, 316852. *Gerbillus garamantis* FMNH 72828. *Gerbillus gerbillus* MVZ 34214, 107722, 34212, 34213. *Gerbillus gleadowi* USNM 353247, 353617, 353622, 369058. *Gerbillus henleyi* MVZ 107720; USNM 472202, 472203, 472204. *Gerbillus hesperinus* USNM 486006, 485964, 486005, 485970. *Gerbillus hoogstraali* USNM 540028, 540038, 540037, 540034. *Gerbillus latastei* USNM 321822, 321813, 321821, 321794. *Gerbillus mauritaniae* USNM 401519, 401522, 401518, 401002. *Gerbillus mesopotamiae* USNM 350442, 350444, 350443, 350450. *Gerbillus muriculus* USNM 141503, 297485, 141504; FMNH 105600. *Gerbillus nanus* MVZ 191952, 191953, 191955, 191958; FLMNH 14577, 25903, 28564, 28562. *Gerbillus nigeriae* USNM 573945, 573944. *Gerbillus occiduus* USNM 540040. *Gerbillus perpallidus* USNM 316820, 316823, 316819, 316822. *Gerbillus poecilops* USNM 321575, 321584, 321577, 321579. *Gerbillus pulvinatus* USNM 500939, 500943, 500940, 500942. *Gerbillus pusillus* USNM 500947, 500946, 500945; FMNH 44419. *Gerbillus pyramidum* MVZ 34208, 107723, 34210; AMNH 119507. *Gerbillus tarabuli* USNM 302165, 302167, 302160, 302218. *Meriones crassus* MVZ 191991; USNM 401159, 401161, 401157. *Meriones erythrourus* FMNH 202109. *Meriones grandis* USNM 473951, 483036, 473866, 474353. *Meriones hurrianae* USNM 369162, 369163, 369161, 369510. *Meriones libycus* MVZ 191968, 191972, 191962, 191963. *Meriones meridianus* MVZ 41227, 41228; AMNH 59702, 59352. *Meriones persicus* MVZ 198812, 198813, 198811, 198819. *Meriones rex* USNM 321715; FMNH 77953, 77955, 77959. *Meriones shawi* USNM 474209, 474187, 474208, 474185. *Meriones tamariscinus* USNM 155457, 155459; AMNH 85369, 85377. *Meriones tristrami* MVZ 183874; USNM 327436, 327438, 327437. *Meriones unguiculatus* MVZ 41229; USNM 240765, 283918, 270551. *Meriones vinogradovi* MVZ 183875; USNM 354663, 354662; FMNH 97405. *Pachyuromys duprasi* FMNH 74976, 89621, 80021, 80048; MVZ 34197; USNM 482421, 321829, 325567, 325569. *Psammomys obesus* AMNH 203215; FMNH 78611, 91277, 91279; MVZ 183877; USNM 482457, 326018, 326025, 341974. *Rhombomys opimus* AMNH 88865, 88868, 88871, 88875; MVZ 41226; USNM 341327, 341329, 341332, 341334. *Sekeetamys calurus* FMNH 101021, 101025, 101024, 101033; USNM 321934, 321928, 321931, 321932. *Tatera indica* AMNH 240846; MVZ 192006, 192007, 192002, 192005; FLMNH 30352, 30266, 30245, 30260. *Taterillus arenarius* USNM 401124, 401978, 401117, 401980. *Taterillus congicus* AMNH 50294, 50295, 50298, 50300. *Taterillus emini* USNM 165288, 299721, 165289, 299718. *Taterillus gracilis* USNM 403445, 438169, 403447, 438165. *Taterillus harringtoni* USNM 483985, 483990, 483998, 483991. *Taterillus lacustris* USNM 378930, 378929, 378925, 378923. *Taterillus pygargus* USNM 376373, 380412, 376311, 380413. Lophiomyinae: *Lophiomys imhausi* USNM 291766, 172694, 184114, 184115. Murinae: *Abeomelomys sevia* AMNH 191963, 191965, 191966, 191964. *Aethomys chrysophilus* MVZ 117532, 117534, 118188, 117531. *Aethomys namaquensis* MVZ 117521, 117524, 117519, 117520. *Anisomys imitator* AMNH 194893, 194894, 194892, 194891. *Apodemus agrarius* MVZ 120896, 120898, 125183, 121103. *Apodemus mystacinus* USNM 327654; MVZ 100019, 72459, 72461. *Apodemus semotus* USNM 261057, 333017, 361053, 333014. *Apodemus speciosus* MVZ 119797; USNM 299360. *Apodemus sylvaticus* FMNH 74411, 74409, 74412; USNM 153235. *Apomys datae* FMNH 188427, 188448, 188280; USNM 574889. *Apomys hylocoetes* FMNH 147871, 147872; USNM 125243, 125244. *Archboldomys luzonensis* USNM 573837, 573835, 573838, 573840. *Arvicanthis neumanni* FMNH 158037; MVZ 101023. *Arvicanthis niloticus* FMNH 105595, 105596, 105597; MVZ 154335. *Bandicota bengalensis* MVZ 181303, 181305; FLMNH 14630, 27590. *Batomys salomonseni* FMNH 147940, 148163, 148170, 148172. *Berylmys bowersi* MVZ 186483, 186484, 186482, 186490. *Bullimus bagobus* USNM 462203, 459923, 462206, 458789. *Bunomys chrysocomus* AMNH 224769, 224767; MVZ 225697, 225810. *Carpomys phaeurus* FMNH 62291. *Chiromyscus chiropus* AMNH 268333; FMNH 32010; USNM 321507, 308218. *Chiropodomys gliroides* AMNH 106684, 106681, 106687; USNM 283681. *Chrotomys gonzalesi* USNM 356290, 458955. *Colomys goslingi* AMNH 55219, 55220; USNM 537872, 375903. *Conilurus penicillatus* AMNH 183587; FMNH 120704; USNM 141486, 141487. *Cremnomys cutchicus* FMNH 35295, 82993, 82994, 82996. *Crunomys melanius* FMNH 147106, 167889. *Dacnomys millardi* FMNH 84892, 76519, 84881; MVZ 186519. *Dasymys*

incomtus AMNH 118839, 118837, 118835; MVZ 88742. *Golunda ellioti* FMNH 83032, 83034, 83036; FLMNH 14613. *Grammomys dolichurus* MVZ 117387, 117389, 117386, 118168. *Grammomys ibeanus* USNM 183754, 162530, 162529, 162528. *Grammomys macmillani* FMNH 73916, 73917, 79469; USNM 299736. *Hapalomys delacouri* FMNH 32463. *Heimyscus fumosus* USNM 585164, 584972, 585169, 585173. *Hybomys univittatus* USNM 84522, 580737, 545844, 580207. *Hydromys chrysogaster* MVZ 119719, 121748, 119419, 129303. *Hylomyscus parvus* USNM 585202, 585208, 584752, 584754. *Hylomyscus stella* FMNH 165219, 165221, 165223; MVZ 196244. *Hyomys goliath* MVZ 129941; 194909, 194899, 194910. *Leggadina forresti* USNM 284270; FMNH 120331, 120330. *Lemniscomys barbarus* USNM 475121, 475161, 475122, 475165. *Lemniscomys striatus* FMNH 17280, 86192, 123809; FLMNH 20537. *Leopoldamys sabanus* FMNH 98587, 98585, 98584; MVZ 186495. *Leptomys elegans* AMNH 158203, 104200, 108447, 104199. *Limnomys sibuanus* FMNH 148174, 147947, 147950, 148175. *Lorentzimys nouhuysi* USNM 585614, 585616, 585612. *Macruromys major* AMNH 152068, 152066, 152069, 152067. *Malacomys longipes* MVZ 196255, 196280, 196254, 196279. *Margaretamys elegans* AMNH 223697, 223696, 225146, 223695. *Mastacomys fuscus* USNM 574492. *Mastomys erythroleucus* FMNH 42353, 42354; MVZ 196261, 196262. *Maxomys bartelsii* USNM 481468, 481516, 481465, 496858. *Maxomys surifer* MVZ 155535, 155537, 155534, 155539. *Melasmothrix naso* AMNH 225087, 225112, 225103, 225110. *Melomys cervinipes* MVZ 134084, 134069, 126567, 126568. *Melomys rufescens* FMNH 54064; USNM 295069. *Mesembriomys gouldii* USNM 284348, 284344, 141489. *Micromys minutus* AMNH 160524; MVZ 123584, 123585, 174890. *Millardia gleadowi* USNM 354414, 413647, 369523, 354414. *Millardia kathleenae* AMNH 163761; FMNH 82944. *Mus booduga* FMNH 35292; USNM 369234, 533854, 533774, 533855. *Mus cervicolor* FMNH 105715, 105714; MVZ 154456, 154455. *Mus cookii* FMNH 105731, 76796, 99769; MVZ 154450. *Mus minutoides* AMNH 168548; MVZ 162503, 162508, 165138, 18295, 117689, 117688; USNM 352800, 352806. *Mus musculus* FLMNH 27595, 14562, 1840, 7588; USNM 298998. *Mus pahari* MVZ 166472, 221555, 221556; USNM 355553. *Mus saxicola* USNM 556247, 556249, 556257, 556248. *Mus spretus* MVZ 226632, 155909, 155911; USNM 486120. *Mus terricolor* USNM 533850, 533851, 398777, 279167. *Mylomys dybowskii* USNM 317996, 183598, 183604, 183608. *Myomyscus brockmani* USNM 183495, 259902, 183502, 162472. *Niviventer confucianus* AMNH 58972; MVZ 174887, 174871, 174888. *Niviventer cremoriventer* USNM 292782, 488957, 292790, 488962. *Niviventer excelsior* USNM 574373, 574372. *Notomys alexis* MVZ 134373; USNM 284363; AMNH 197502, 197504. *Notomys cervinus* USNM 284352, 284359; AMNH 153491, 153492. *Notomys fuscus* MVZ 124313, 124312, 124314, 124315. *Oenomys hypoxanthus* USNM 183631, 220534, 437349, 297526. *Otomys angoniensis* USNM 437517, 382382, 318084, 382383. *Otomys denti* USNM 381484, 381486, 259555, 340925. *Parotomys brantsii* AMNH 168509, 168510;

MVZ 117756, 118405. *Parotomys littledalei* MVZ 81577; USNM 343927, 343936, 343923, 256963. *Paruromys dominator* AMNH 225744, 225742; MVZ 225784, 225788. *Phloeomys cumingi* FLMNH 22381. *Pogonomys loriae* USNM 357495, 357496. *Pogonomys macrourus* MVZ 140443, 138620, 140447, 140450. *Praomys jacksoni* AMNH 82454; MVZ 196286, 196289, 196287. *Praomys misonnei* FMNH 149595, 149597, 149598, 149601. *Praomys tullbergi* MVZ 133098, 133099; USNM 463056. *Pseudohydromys ellermani* MVZ 129794, 129796, 129798. *Pseudomys australis* AMNH 65998; MVZ 134044, 134115, 133681. *Pseudomys hermannsburgensis* AMNH 197431, 197433, 220112, 220113. *Rattus exulans* FLMNH 27816, 28982, 30104; USNM 321152. *Rattus norvegicus* FLMNH 3945, 12719, 39452, 2885. *Rattus praetor* USNM 277303, 290540, 277304, 277067. *Rattus rattus* USNM 356509, 465, 1250, 468. *Rattus sordidus* MVZ 133641, 133606, 133637, 133639. *Rattus tiomanicus* FMNH 171919, 171920, 171917; USNM 590331. *Rattus verecundus* USNM 357439, 357437, 357431, 357438. *Rattus villosissimus* AMNH 153476, 153495, 153475, 153477. *Rhabdomys pumilio* MVZ 88824, 88823, 88820, 117468. *Rhynchomys isarogensis* USNM 573906, 573905, 573912, 573911. *Stenocephalemys albipes* USNM 515391, 516174, 516155, 516179. *Stochomys longicaudatus* FMNH 29471, 29472, 74223; MVZ 196264. *Sundamys muelleri* USNM 113035, 115593, 104838, 121764. *Tarsomys apoensis* FMNH 148177, 148176; USNM 144619. *Uromys caudimaculatus* MVZ 175371, 175372, 140440, 134112. *Vandeleuria oleracea* AMNH 242257; USNM 279309, 277861, 279310. *Zelotomys hildegardeae* USNM 183912, 183913, 181804, 183911. *Zelotomys woosnami* USNM 428770, 428771, 428772, 470118. *Zyzomys argurus* USNM 284323, 578555, 284328, 384336. Nesomyidae: Cricetomyinae: *Beamys hindei* USNM 183107, 183109, 183103, 183108. *Cricetomys gambianus* FMNH 128237; MVZ 196236, 196237; FLMNH 29051. *Saccostomus campestris* MVZ 118335, 118371, 118364, 118365. Delanymyinae: *Delanymys brooksi* AMNH 181210, 181208, 181209; FMNH 148417. Dendromurinae: *Dendromus insignis* USNM 164387, 184067, 164392, 164454. *Dendromus mesomelas* MVZ 117690. *Dendromus nyasae* FMNH 196686, 191596, 191597, 191598. *Malacothrix typica* USNM 343711, 423199, 343708, 423204. *Steatomys krebsi* FMNH 153193. *Steatomys parvus* USNM 367225, 428962, 295978, 164468. Petromyscinae: *Petromyscus collinus* AMNH 165437, 165438, 165439, 165408; USNM 424617, 452334, 452406, 452433. Mystromyinae: *Mystromys albicaudatus* USNM 468440, 422538, 422540, 468445. Nesomyinae: *Brachytarsomys albicauda* AMNH 100692; MVZ 217015; USNM 449215, 449214. *Brachyuromys betsileoensis* AMNH 100802; MVZ 216974; USNM 328818, 328815. *Eliurus minor* USNM 448974, 578678, 328827, 449246. *Eliurus tanala* USNM 448986, 449251, 448987, 449253. *Gymnuromys roberti* FMNH 5632, 151694, 151695; MVZ 221230. *Hypogeomys antimena* AMNH 119705. *Macrotarsomys bastardi* USNM 328795, 328802, 328796, 578717. *Monticolomys koopmani* AMNH 275217, 275214. *Nesomys rufus* AMNH 100679; MVZ 217006; USNM 449239,

449245. *Voalavo gymnocaudus* FMNH 156162, 159648, 159725, 159727. Platacanthomyidae: Platacanthomyinae: *Typhlomys cinereus* AMNH 84762, 84769, 84761; FMNH 39131. Spalacidae: Myospalacinae: *Eospalax fontanierii cansus* FMNH 19070, 19069. *Myospalax aspalax* FMNH 49900, 49901. Spalacinae: *Spalax ehrenbergi* FMNH 101009, 101010, 101014, 101011. Rhizomyinae: *Cannomys badius* FMNH 104207, 104211, 104212; MVZ 183902. *Rhizomys pruinosus* FMNH 84849; MVZ 186543, 186544, 186548. Tachyoryctinae: *Tachyoryctes splendens* MVZ 163968, 183904, 183908, 183907.

Sciuromorpha.—Gliridae: Leithiinae: *Eliomys melanurus* USNM 475706, 302274, 475705, 342024. *Eliomys quercinus* MVZ 154697; USNM 103031, 103032, 152768. Graphiurinae: *Graphiurus ocularis* AMNH 168333, 168332, 89052. Sciuridae: Xerinae: *Ammospermophilus harrisii* USNM 33713; FLMNH 2508; FMNH 14956, 4873. *Ammospermophilus interpres* USNM 18154, 20077, 108389, 108928. *Ammospermophilus leucurus* USNM 53221; FLMNH 4744, 5383, 2494. *Ammospermophilus nelsoni* USNM 31273, 129865, 54629, 127152. *Atlantoxerus getulus* USNM 470900, 470895, 476815, 476821. *Spermophilus fulvus* USNM 369544; AMNH 206566, 176239; FMNH 96891. *Spermophilus mexicanus* USNM 33546, 34118, 33549, 34123. *Spermophilus mohavensis* USNM 15975, 135838, 28740, 192753. *Spermophilus pygmaeus* USNM 251636, 251637; AMNH 87089, 87090. *Spermophilus spilosoma* USNM 247654, 35079, 35077, 350800. *Spermophilus tereticaudus* USNM 96984, 33762, 138610, 33754. *Spermophilus variegatus* USNM 117529, 117602, 97156, 117604. *Xerus erythropus* USNM 421581, 453006, 453008, 453009. *Xerus inauris* USNM 368056, 368059, 259785, 368058. *Xerus princeps* USNM 379848, 379847; AMNH 86479.

APPENDIX II

Collected measurements.—The following measurements were collected for each specimen in Appendix I.
Ventral cranial characters.—1) Skull length (SL) is a common measure of skull size taken from the anterio-medial most inferior border of the foramen magnum to the anterio-medial most border of the premaxillaries. It is also known as the basilar length and is somewhat shorter than the other common size measurement, the condylobasal length. 2) Skull width (SW) is the maximum width of the skull perpendicular to SL. This measurement, also known as the zygomatic breadth/width, captures the greatest distance across zygomatic arches. 3) Incisor width (IW) measured at the insertion of the incisors to the premaxilla (widest part). 4) Diastema length (DL) measured at the alveoli. 5) Molar tooth row length (ML) measured at the occlusal region. 6) First molar width (MW) measured at the occlusal region. 7) Pterygoid region length (PR) measured as the widest distance across the structure. 8) Basicranial width (MB) corresponds to the anterior width of the basioccipital. 9) Basioccipital length (BO) is the anterio-posterior extent of the basioccipital. 10) Bulla length (BL) is the maximum length

of the auditory bulla from the anterior point of insertion into the basioccipital to the posterior-most of the tympanic bulla, not including the mastoid part of the auditory bulla. 11) Bulla width (BW) approximately perpendicular to BL and across the auditory meatus. 12) Condyle breadth (CB) measures the widest distance across the occipital condyles. Measurements (2)–(10) and (12) follow Steppan (1997), measurements (1) and (10) follow Squarcia et al. (2007), and measurements (1), (2), and (10) follow Francescoli et al. (2012). Ventral cranial measurements are depicted in Supplementary Data SD5.
Lateral cranial characters.—13) Incisor depth (ID) is the anterio-posterior extent of the incisors. 14) Incisor height (IH) is the longest distance from the tip of the incisors to their insertion into the premaxillaries. 15) Rostral depth (RD) is the deepest part of the rostrum. 16) Lateral molar row length (LML) is the same as ML, viewed laterally (measured again to calculate averages; see above). 17) First molar height (MH) is the maximum height of the 1st molar. 18) Maximum lateral bulla length (LBL) is the same as BL, viewed laterally (measured again to calculate averages). 19) Bulla height (BH) is approximately perpendicular to the plane defined by BL and BW across the auditory meatus (perpendicular to LBL). Measurements (13), (15), and (16) follow Steppan (1997), and measurements (18) and (19) follow Francescoli et al. (2012). All lateral cranial characters are depicted in Supplementary Data SD7.
Dorsal cranial characters.—20) Nasal breadth (NB) is the widest distance across the nasals. 21) Nasal length (NSL) is the anterio-posterior extent of the nasals. 22) Interorbital breadth (IOB) is the minimum distance between the upper edges of the orbits across the dorsal side of the skull. 23) Dorsal skull width (DSW) is also known as the zygomatic breadth and is another measure of skull width similar to SW. 24) Dorsal skull length (DSL) another measure of skull length similar to SL. Measurements (20)–(24) follow Steppan (1997), measurement (21) also follows Agrawal (1967), and measurement (23) also follows Francescoli et al. (2012). All dorsal cranial characters are depicted in Supplementary Data SD8.
Occlusal mandible characters.—25) Lower incisors width (LIW) is the width across both lower incisors; in mandibles disarticulated at the symphysis, the width across 1 incisor was multiplied by 2. 26) Incisor length (IL) is the maximum length of the incisors. 27) Jaw diastema length (JDL) is the distance between the molar tooth row and the incisor at the alveoli. 28) Jaw molar tooth row length (JML) measured at the occlusal region. 29) Jaw 1st molar width (JMW) measured at the occlusal region. 30) Total jaw length (TJL) is the distance from the anterior tip of the incisor to the posterior extreme of the jaw at the condyloid process. Measurements (25) and (26) follow Ojeda et al. (1999), measurement (26) also follows Agrawal (1967), measurement (27)–(29) follow Steppan (1997), and measurement (30) follows Ndiaye et al. (2012). All occlusal mandible characters are depicted in Supplementary Data SD10.
Lateral mandible characters.—31) Jaw incisor depth (JID) is the anterio-posterior extent of the incisors. 32) Incisor length (IL2) is the maximum length of the incisors viewed from the lateral side of the mandible. 33) Jaw length measurement

I (JLS) from the incisor to the angular process, similar to TJL. 34) Moment arm of the masseter (MAM) is the distance from angular to condyloid process. 35) Jaw length measurement II (JLB) is the distance from the incisor to the condyloid process, similar to TJL. 36) Jaw molar 1 height (JMH) is the maximum height of the 1st molar of the mandible. Measurements (31), (33), and (34) follow Steppan (1997), measurement (32) follows Ojeda et al. (1999), and measurement (35) follows Ndiaye et al. (2012). All lateral mandible characters are depicted in Supplementary Data SD11.

Derived characters.—37) Average jaw length (AJL) is the average of TJL, JLS, and JLB. 38) Average incisor length (AIL) is the average of IL and IL2. 39) Average skull length (ASL) is the average of SL and DSL. 40) Average skull width (ASW) is the average of SW and DSW. 41) Average molar length (AML) is the average of ML and LML. 42) Average bulla length (ABL) is the average of BL and LBL. 43) Bulla index (BI) is calculated as the ratio of ABL to ASL. 44) Bulla volume (BV) is the 3D

measure calculated following Schleich and Vasallo (2003) and Francescoli et al. (2012) using the formula of an elliptical cone

where:
$$BV = \frac{(\pi)\left(\dfrac{ABL}{2}\right)\left(\dfrac{BW}{2}\right)(BH)}{3}$$

Similar to BI, this character only accounts for the inflation of the tympanic portion of the bulla and not the mastoid portion of the bulla. 45) Nasal index (NI) is a measure of the shape of the nasals calculated as the ratio of NB to NSL. 46) Nasal volume (NV) is an estimate of shape/size of the nasal passages/turbinates calculated as the product of NB, NSL, and RD. 47) Lower incisor index (LII) is the ratio of LIW to AIL and estimates the shape of the lower incisors. Measurements (43) and (47) follow Ojeda et al. (1999), measurement (43) also follows Squarcia et al. (2007), measurement (44) follows Schleich and Vasallo (2003) and Francescoli et al. (2012), and measurement (45) is a standard anthropological measurement.